UNIVERSITÀ POLITECNICA DELLE MARCHE
Repository ISTITUZIONALE

Living and dead foraminiferal assemblages of the last decades from Kveithola Trough: Taphonomic processes and ecological highlights

This is the peer reviewd version of the followng article:

Original
Living and dead foraminiferal assemblages of the last decades from Kveithola Trough: Taphonomic processes and ecological highlights / Gamboa-Sojo, V.M., Husum, K., Caridi, F., Lucchi, R.G., Bensi, M., Kovačević, V., Sabbatini, A., Langone, L., Dominiczak, A.T., Povea, P., Morigi, C.. - In: MARINE MICROPALEONTOLOGY. - ISSN 0377-8398. - ELETTRONICO. - 166:(2021). [10.1016/j.marmicro.2021.102014]

Availability:
This version is available at: 11566/291005 since: 2025-01-29T12:47:36Z

Publisher:

Published
DOI:10.1016/j.marmicro.2021.102014

Terms of use:

The terms and conditions for the reuse of this version of the manuscript are specified in the publishing policy. The use of copyrighted works requires the consent of the rights' holder (author or publisher). Works made available under a Creative Commons license or a Publisher's custom-made license can be used according to the terms and conditions contained therein. See editor's website for further information and terms and conditions.
This item was downloaded from IRIS Università Politecnica delle Marche (https://iris.univpm.it). When citing, please refer to the published version.

(Article begins on next page)

05 October 2026

Living and Dead foraminiferal assemblages of the last decades from Kveithola Trough: taphonomic processes and ecological highlights.

Highlights

Monitoring recent short and long-term climatic variations in the Kveithola Trough.

Comparison of the living and dead foraminiferal assemblages

Integration of the foraminifera, oceanographic and sedimentological data.

Analysis of taphonomic processes using the living and dead foraminiferal assemblages

Evaluation of bias on the paleocological reconstruction due to taphonomy

Living and Dead foraminiferal assemblages of the last decades from Kveithola Trough: taphonomic processes and ecological highlights.

Viviana Maria Gamboa Sojo [a. b. c.], Katrine Husum [d.], Francesca Caridi [e.], Renata G. Lucchi [f. g.], Manuel Bensi [f.], Vedrana Kovacevic [f.], Anna Sabbatini [e.], Leonardo Langone [h.], Aleksander Tadeusz Dominiczak [i.], Patricia Povea [j.], Caterina Morigi [a. k.]

a. Department of Earth Sciences. University of Pisa, Pisa, Italy
b. Department of Earth Sciences. University of Florence, Florence, Italy
c. Department of Earth Sciences. University of Costa Rica, San Jose Costa Rica
d. NPI Norwegian Polar Institute, Fram Centre, Tromsø, Norway
e. Department of Life and Environmental Sciences, Polytechnic University of Marche, Ancona, Italy
f. National Institute of Oceanography and Applied Geophysics (OGS), Trieste, Italy.
g. Centre for Arctic Gas Hydrate, Environment and Climate (CAGE), UiT-The Arctic University of Norway, Tromsø, Norway
h. Institute of Polar Sciences, Italian National Research Council (CNR-ISP), Bologna, Italy
i. Institute of Geology, Adam Mickiewicz University in Poznan, Poland
j. University of Barcelona, Barcelona Spain
k. Stratigraphy Department, Geological Survey of Denmark and Greenland (GEUS), Copenhagen, Denmark

Living and Dead foraminiferal assemblages of the last decades from Kveithola Trough: taphonomic processes and ecological highlights.

Abstract

We examine the living and dead benthic foraminiferal assemblages from the topmost 10cm (using 150 µm sieve fraction) of three sedimentological short records collected in the Kveithola Trough (northwest Barents Sea). Our aim is to reconstruct the environmental variations of the last decades, connected to the interaction among the North Atlantic and the Arctic water masses. Our samples are collected at water depths between 150 and 380 m during the Eurofleets2-BURSTER oceanographic cruise, on board of the R/V Polarstern (June 2016).

In the Cell Tracker Green (CTG) labelled living foraminiferal fauna, the main species are *Pullenia bulloides*, *Globobulimina auriculata*, and *Nonionellina labradorica*, while in the dead assemblages the main species are *Cassidulina neoteretis*, *Cibicidoides lobatulus*, and *Cassidulina reniforme* (outer, inner, and shelf stations, respectively). The dead foraminiferal assemblages show no significant traceable environmental changes in the Kveithola Trough area occurred during the last *ca.* 100 years. Conversely, the living foraminiferal fauna shows that this area is subject to variations related to circulation changes and organic matter burial in sediments, to which the biota adapts quickly. Moreover, the species that are only observed in the dead foraminiferal assemblages and not in the living CTG-labelled foraminiferal assemblages (e.g. *C. reniforme*) are typical of colder water and highlight the ongoing warming of the Arctic area. We find that the preservation of foraminiferal tests may bias the paleontological results. The agglutinated tests are often disintegrated, and the delicate calcareous ones are broken. The environmental conditions (style of sedimentation, bottom currents, interaction with other communities) can weaken the foraminiferal tests and make them prone to breakage or dissolution.

Keywords Living vs. dead benthic foraminifera; taphonomic processes; oceanographic processes; Kveithola Trough (Barents Sea); Arctic.

Living and Dead foraminiferal assemblages of the last decades from Kveithola Trough: taphonomic processes and ecological highlights.

Viviana Maria Gamboa Sojo [a. b. c.], Katrine Husum [d.], Francesca Caridi [e.], Renata G. Lucchi [f. g.], Manuel Bensi [f.], Vedrana Kovacevic [f.], Anna Sabbatini [e.], Leonardo Langone [h.], Aleksander Tadeusz Dominiczak [i.], Patricia Povea [j.], Caterina Morigi [a. k.]

a. Department of Earth Sciences. University of Pisa, Pisa, Italy
b. Department of Earth Sciences. University of Florence, Florence, Italy
c. Department of Earth Sciences. University of Costa Rica, San Jose Costa Rica
d. NPI Norwegian Polar Institute, Fram Centre, Tromsø, Norway
e. Department of Life and Environmental Sciences, Polytechnic University of Marche, Ancona, Italy
f. National Institute of Oceanography and Applied Geophysics (OGS), Trieste, Italy.
g. Centre for Arctic Gas Hydrate, Environment and Climate (CAGE), UiT-The Arctic University of Norway, Tromsø, Norway
h. Institute of Polar Sciences, Italian National Research Council (CNR-ISP), Bologna, Italy
i. Institute of Geology, Adam Mickiewicz University in Poznan, Poland
j. University of Barcelona, Barcelona Spain
k. Stratigraphy Department, Geological Survey of Denmark and Greenland (GEUS), Copenhagen, Denmark

Corresponding authors: Viviana Maria Gamboa Sojo, Caterina Morigi

E-mail address: vivianamaria.gamboasojo@unifi.it , caterina.morigi@unipi.it

Abstract

We examine the living and dead benthic foraminiferal assemblages from the topmost 10cm (using 150 µm sieve fraction) of three sedimentological short records collected in the Kveithola Trough (northwest Barents Sea). Our aim is to reconstruct the environmental variations of the last decades, connected to the interaction among the North Atlantic and the Arctic water masses. Our samples are collected at water depths between 150 and 380 m during the Eurofleets2-BURSTER oceanographic cruise, on board of the R/V Polarstern (June 2016).

In the Cell Tracker Green (CTG) labelled living foraminiferal fauna, the main species are *Pullenia bulloides*, *Globobulimina auriculata*, and *Nonionellina labradorica*, while in the dead assemblages the main species are *Cassidulina neoteretis*, *Cibicidoides lobatulus*, and *Cassidulina reniforme* (outer, inner, and shelf stations, respectively). The dead foraminiferal assemblages show no significant traceable environmental changes in the Kveithola Trough area occurred during the last *ca.* 100 years. Conversely, the living foraminiferal fauna shows that this area is subject to variations related to circulation changes and organic matter burial in sediments, to which the biota adapts quickly. Moreover, the species that are only observed in the dead foraminiferal assemblages and not in the living CTG-labelled foraminiferal assemblages (e.g. *C. reniforme*) are typical of colder water and highlight the ongoing warming of the Arctic area. We find that the preservation of foraminiferal tests may bias the paleontological results. The agglutinated tests are often disintegrated, and the delicate calcareous ones are broken. The environmental conditions (style of sedimentation, bottom currents, interaction with other communities) can weaken the foraminiferal tests and make them prone to breakage or dissolution.

Keywords Living vs. dead benthic foraminifera; taphonomic processes; oceanographic processes; Kveithola Trough (Barents Sea); Arctic.

1. Introduction.

Polar regions are extremely sensitive areas to long-term climatic variations, which include both natural and anthropogenic influences. As indicated in the IPCC (Intergovernmental Panel on Climate Change) 2019 report, these changes include variations in the Arctic temperature and sea ice extent, producing alterations in the ocean salinity and primary production, and extreme weather conditions around the world (precipitations, droughts, heat, and cyclones; Solomon et al., 2007). The sea ice extent and the seasonal/interannual variations of temperature, albedo, productivity, etc., principally influence the Arctic Ocean (Serreze et al., 2007; Screen and Simmonds, 2010a; Comiso and Hall, 2014; Lind et al., 2018). The marginal Barents Sea is located south of this area and is characterised by two main climatic regions, the cold sea ice covered area in the north and the warmer and productive area in the south (Loeng, 1991; Screen and Simmonds, 2010b; Smedsrud et al., 2013; Lind et al., 2018).

The Kveithola glacial trough system in the NW Barents Sea corresponds to a complex geomorphological environment located at the sea ice limit and influenced by the interaction of different water masses (Atlantic and Arctic waters) (Aagaard, 1989; Loeng, 1991; Vinje and Kvambekk, 1991; Loeng et al., 1997; Orvik and Niiler, 2002; Maslowski et al., 2004; Smedsrud et al., 2013). Quaternary climate studies of the Barents Sea, based on sedimentary data set, indicate a general increase in the sea temperature (Duplessy et al., 2001; Rebesco et al., 2011; Rüther et al., 2012; Groot et al., 2014; Dijkstra et al., 2017a). In particular, some papers highlighted the variation in the inflow of the warm Atlantic water into the Barents Sea during the Holocene (Duplessy et al., 2001; Sarnthein et al., 2003; Ślubowska-Woldengen et al., 2007; Groot et al., 2014).

Some of these paleoclimatic studies have been based on benthic foraminiferal records from the Barents Sea (e.g. Sarnthein et al., 2003; Ślubowska-Woldengen et al, 2007; Groot et al., 2014; Dijkstra et al.,

2017a). Benthic foraminifera are important (paleo-) ecological indicators due to their wide diffusion in the oceans, and their good potential preservation in the fossil record. The distribution of the foraminiferal living assemblages in the Barents Sea is strongly related to water mass characteristics, e.g. temperature and available nutrition (e.g. Saher et al., 2012; Dijkstra et al., 2013). Studies that compare the living and dead benthic foraminiferal assemblages point to some preservation issues (transport, bioturbation, dissolution and/or broken test), which may bias the interpretation of the fossil record (e.g., Hald and Korsun, 1997; Wollenburg and Mackensen, 1998; Dijkstra et al., 2017a; Dijkstra et al., 2017b).

Based on this premise, the objective of this study is threefold: 1) to discuss the distribution of living foraminiferal assemblages in the Kveithola Trough and their relation to the local oceanographic processes; 2) to evaluate the taphonomic processes that bias the ecological interpretation in a high-latitude environment; and 3) to reconstruct environmental variations of the last decades on the basis of the dead foraminiferal assemblages. To reach these objectives we have analysed oceanographic, geomorphological, and sedimentological data as potential drivers of the living and dead foraminiferal assemblages.

2. Bathymetric features and oceanographic patterns of the study area

The Kveithola Trough located in the NW Barents Sea, is an abrupt bathymetric feature about 100 km long and 13 km wide, with a water depth ranging from 100 to 400 m (Fohrmann et al., 1998; Rüther et al., 2012) (Fig. 1). The longitudinal profile of the trough is markedly staircase-like, composed of five transverse ridges located about 15 km apart from each other, and interpreted as Grounding Zone Wedges (*sensu* Dowdeswell and Fugelli, 2012) that testify the episodic mode of the retreat of former ice stream(s) after Last Glacial Maximum (Rebesco et al., 2011; Bjarnadóttir et al., 2013). Other prominent seafloor

morphological features are mega-scale glacial lineations generated by grounded ice sheet advance (Rebesco et al., 2011), and two mounded depocentres with an associated moat developing along the northern margin of the glacial trough that are interpreted as a sediment drift complex (Rebesco et al., 2016) (Fig. 1). The northernmost area is crossed by a pronounced moat, that channelize dense bottom currents crossing the trough from the inner (East) to the outer (West) area delivering sediments to the shelf break and to the drift system (Rebesco et al., 2016; Lantzsch et al., 2017) (Fig. 1). Another important element in the area is a system of faults in the inner part of the Kveithola Trough and the northern part of the shelf evidenced by Mau et al. (2017). Along this fault system a local evidence of hydrocarbon seepage activity is detected (station 21) (Lucchi et al., 2016; Mau et al., 2017; Bazzaro et al., 2020), driving macrofaunal diversity and trophic conditions (Caridi et al., 2019).

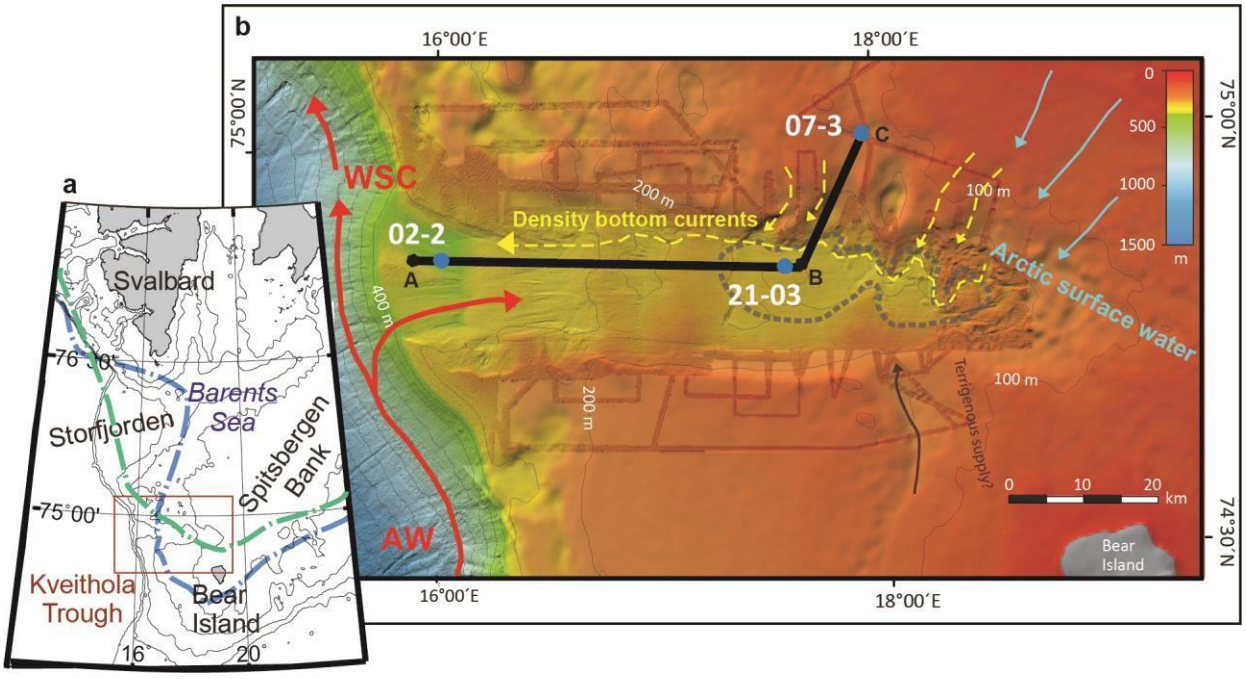

Fig. 1. (a) Overview map showing the location of the Kveithola Trough in the NW Barents Sea. The blue dot-dashed line shows the position of the Polar Front (Harris et al., 1998). The green dot-dashed line

represents the mean of the maximum sea ice extent from 1980-2010 (National Snow and Ice Data Centre (NSIDC, https://nsidc.org/). (b) Bathymetric map of Kveithola Trough. The black ABC line shows the location of the bathymetric profile displayed in Fig. 7. The blue filled circles indicate the cored sites. The red arrows represent the path of the West Spitsbergen Current (WSC), whereas the light blue arrows indicate the input of the Arctic surface water. The yellow dashed arrows indicate the direction of density bottom currents. The grey dashed polygon on the inner Kveithola Trough delimits the sediment drift complex, and the dark brown arrow indicates a possible terrigenous supply coming from the south (Lantzsch et al., 2017).

Relatively fresh, cold Arctic waters (ArW) and warm, salty Atlantic waters (AW) constantly interact within the Kveithola Trough (Fig. 1). ArW flow from the Arctic Ocean and influence the northern-eastern part of the trough (Aagaard et al., 1985; Aagaard, 1989; Loeng, 1991; Orvik and Niiler, 2002); whereas the warm and saline AW are transported in the area by the West Spitsbergen Current (WSC), representing the northernmost branch of the North Atlantic Current proceeding from south along the bathymetric contour (Aagaard et al., 1973; Aagaard et al., 1981; Aagaard, 1989; Vinje and Kvambekk, 1991; Loeng et al., 1997; Maslowski et al., 2004; Smedsrud et al., 2013). The Kveithola Trough is seasonally influenced by the presence of sea ice during the winter seasons as it is on the southern limit of the maximum ice extent during late winter, around March-April (Fig. 1). However, the sea-ice extent in the Barents Sea suffers from a strong interannual variability as well as a progressive long-term reduction (www.mosj.no). Decadal oscillations of the sea-ice extent in the Arctic and hence in the Barents Sea seem to be linked to large scale climatic patterns such as the Pacific Decadal Oscillation, the North Pacific Gyre Oscillation, and the North Atlantic Oscillation-like atmospheric pressure conditions (see e.g., Koenigk et al., 2009; Yang et al., 2020).

3. Materials and methods

The geological and oceanographic dataset presented in this work was collected during the Eurofleets 2- BURSTER cruise on-board the R/V Polarstern (Expedition PS99-1a), Bremerhaven-Longyearbyen, June 13– 23, 2016 (Lucchi et al., 2016). The data were acquired over the Kveithola area between 19th and 20th June 2016.

3.1 Oceanographic data set

3.1.1 Thermohaline data

Temperature (T, °C), salinity (SAL, PSU) and dissolved oxygen (DO, ml l^{-1}), were recorded throughout the water column by means of a SeaBird 911-plus CTD (Conductivity-Temperature-Depth) mounted on the SBE 32 Carousel Water Sampler (Rosette) equipped with 24 Niskin Bottles (12-liter capacity). The DO concentration was also determined in parallel on water samples taken at discrete depths from the Niskin bottles using the Winkler method (Carpenter, 1965).

Potential temperature (θ, °C) was calculated from each original in-situ data set using the toolbox TEOS-10 (http://www.teos-10.org/software.htm). Some data were plotted using Ocean Data View (ODV; Schlitzer, 2021).

3.1.2 Horizontal currents

The vertical distributions of horizontal currents were obtained from a vessel mounted Acoustic Doppler Current Profiler (vmADCP, Teledyne RDI 150 kHz Ocean Surveyor configured in 'Narrowband' mode). The water column was divided into 80 cells with 4 m size obtaining data in the range from approximately 10 m to 320 m depth. However, the vmADCP cannot sample more than 80–90 % of the water column within its

operating range, so it does not allow for measuring currents close to the seafloor. In our study area, the blanking distance amounts to about 40-50 m above the seafloor.

3.1.3 Satellite images

To identify the southern limit of the sea ice extent during winter, we used satellite images that are freely available from the NASA Worldview application (https://worldview.earthdata.nasa.gov), part of the NASA Earth Observing System Data, and Information System (EOSDIS). The spatial imagery resolution is 250 m, and the temporal resolution is daily.

3.2 Geological data set

Multicore samples were collected using a video-guided multi-corer (TV-MUC), along a west- east (outer- inner) transect in the Kveithola Trough, at water depths ranging from 376 m to 159 m (Fig. 1; Tab. 1). Two cores from each deployment were selected. One core was sampled on-board for living benthic foraminiferal analysis, and a second core was opened, described, subsampled on-board and used for radiometric dating and analysis of grain size and dead benthic foraminifera. In this study, we focus on the upper 10 cm of the sediment cores, which were sliced at every 0.5 cm for the upper 2 cm and at every 1 cm in the interval between 2-10 cm below seafloor (bsf).

Tab. 1. Location and water depth of the multi-cores, and average values (0-10 cm bsf) of physical and biochemical characteristics. BAC = bioavailable carbon, and algal fraction of BPC, Lipid and CHO = carbohydrates (from Caridi et al., 2019).

Station	Coordinates	Water depth (m)	Mean grain size (phi)	BAC (mg/g)	Algal fraction of bpc%	Lipid (mg/g)	CHO (mg/g)
02	74° 51.49' N, 16° 05.84' E	376	4	2.52	10.45	0.49	2.34
21	74° 52.40' N; 17° 21.60' E	306	5	6.23	17.27	1.27	7.00
07	4° 59.69' N; 17° 59.72' E	159	6	5.97	34.13	1.72	7.02

3.2.1 Grain size analyses

Grain size analyses were performed using a Coulter-counter laser Beckman LS-230 scanning the 0.04-2000 µm fraction with 0.004 µm resolution. The sediments were treated with peroxide water to eliminate the organic matter, and the disaggregated sediments were suspended into a 0.1% sodium-hexametaphosphate solution to prevent sediment flocculation. The samples were left 3 minutes into an ultrasonic bath prior to measurement. The results were classified according to Friedman and Sanders (1978) grain-size scale.

3.2.2 ^{210}Pb and ^{137}Cs analysis

Sedimentation rate (SR) for the three cores was determined on the basis of short-lived radionuclides (^{210}Pb and ^{137}Cs). Samples of 20 gram of sediment were homogenised, packed in vials of uniform geometry and left for three weeks before they were measured for 24 h with a high-purity germanium detector (Canberra BE3830). The ages and SR were calculated on the basis of constant flux-constant sedimentation model (CF-CS) (Robbins and Edgington, 1975), and the best-fit linear regression was applied to the core region with more regularly decreasing activity, thus discarding data from the surface mixed layer or from

subsurface peaks. Identification of peaks in ^{137}Cs activity helped to support the depth-age modelling (Ritchie and McHenry, 1990; Pittauerová, 2013).

3.2.3 Living and Dead foraminiferal data

For the living foraminiferal analysis, the sediment slices were incubated in a refrigerator for 12-15 hours in Cell Tracker Green CMFDA (CTG), and then fixed in 10% formalin buffered with sodium borate solution, following the staining procedure as indicated in Pucci et al. (2009). CTG is a non-terminal, non-fluorescent probe that can be cleaved by non-specific esterase common to living cells, producing a fluorescent compound, fluorescein, visible using a fluorescent microscope. The requirement of esterase activity means that a cell must be alive to produce fluorescence (Bernhard et al., 2006). In the laboratory, the sediment samples were sieved through 63, 150 and 500 µm mesh, and kept wet while the whole amount of living specimens were hand-sorted in water using a fluorescence binocular microscope from both size fractions. For this study, we used the data obtained from the coarse fraction (up to 150 µm), besides we did not consider the soft-shelled foraminifera because these taxa are not preserved in the thanatocoenosis, as their organic tests degrade and disappear as soon as they die. The soft-shelled foraminifera were counted only in the living microfauna, found to constitute about the 35% of the total living assemblages. Such data set will be discussed in a future study focused on the ecology of soft-shelled taxa (Caridi et al., in preparation). To compare living to dead foraminiferal data, we normalised the values of the living foraminifera for volume of sediment, in gram of sediment, using the following formula:

$m=\rho V$ where: m = mass of the sediment in gram, ρ = density in g/c.c. and V = volume in c.c.

The samples for analysis of dead foraminiferal assemblages were dry-weighed and wet-sieved using the mesh size of 63 µm. The sample was then dry-sieved at 150 and 500 µm and analysed for the dead benthic foraminiferal assemblages, while the finer size fractions (63-150 µm) were stored for future studies. At

least 300 specimens were picked and identified at species level. For each sample, both living and dead foraminifera were mounted on Plummer cells. The identification at the species level was performed following the taxonomy by Ellis and Messina (1940-1978), Loeblich and Tappan (1953, 1988), Feyling-Hanssen et al. (1971), Wollenburg and Mackensen (1998) and Holbourn et al. (2013). Eventually, some species with similar ecological preferences and belonging to the same genus were grouped together. We identified *Buccella frigida* and *Buccella inusitata,* grouped as *Buccella* spp.*; Islandiella norcrossi* and *Islandiella helenae,* grouped as *Islandiella* spp.; *Reophax scorpiurus* and *Reophax fusiformis,* grouped as *Reophax* spp. Rotaliida spp. comprises a group of species belonging to the same order that we have not been able to identify, since their apertural areas are broken making further identification impossible (Plate 2). The agglutinated broken tests do not allow the identification at the species level and in some cases preclude their recognition at the genus level (Plate 2). The degree of damage of a test or the percentage of broken agglutinated tests was not possible to quantify. No further identification was attempted, as it is not possible to recognise one individual test by the number of broken pieces found in a sample (De Stigter et al., 1999). Species with a relative abundance ≥5% in the dead and living assemblages are considered as main species.

Living and dead ratios were calculated to compare the living and dead proportions of species (Jorissen and Wittling, 1999; Duros et al; 2012; Dessandier et al, 2018):

l/(l+d) where: l = % of living foraminifera and d = % of dead foraminifera

The diversity indices, number of species (S), dominance (D) and Shannon (H) index, were calculated using the software PAST (Hammer et al., 2001).

4. Results

4.1 Water masses properties and ocean current variability

The horizontal and vertical distribution of the physical and biogeochemical properties have been investigated along four N-S oriented sections, two of which went through (or close to) the stations where the sediment samples were collected and hence are presented here (Fig. 2). We have distinguished two main water masses in the Kveithola Basin in June 2016. The relatively warm and saline AW with $\theta > 4.50$ °C and SAL > 35.10 and colder and fresher water originating from the Barents Sea and the northern shelves with $\theta < 4.00$ °C and SAL < 35.00. Dissolved oxygen (DO) ranges from 4 to 7 ml/l in the study area. The lower DO values are primarily associated with the AW and higher values with the shelf waters (Fig. 2). Generally, potential temperature salinity are higher in the upper layers with the values 4.00 - 6.95 °Cand 34.80 - 35.15 (Fig. 2). Below 200 m water depth there is a core of cold (<4.00 °C), fresh (minimum *ca.* 34.90) and oxygenated water. The outermost S-N transect (S1) is characterised by a more evident AW signal, than the inner transect S3. Along the transect S3, passing near station 21 and above station 07, the frontal separation between AW and shelf waters become sharper, and shelf waters extend from the surface down to the bottom in the northern part of the section (Fig. 2). The near-bottom distributions of potential temperature and salinity reveal higher values (4.30–5.00 °C and 35.03–35.10) in the southern deep part of the study region than in the northern part (Fig. 3). The concentrations of DO are in contrast higher in the north-eastern part of Kveithola.

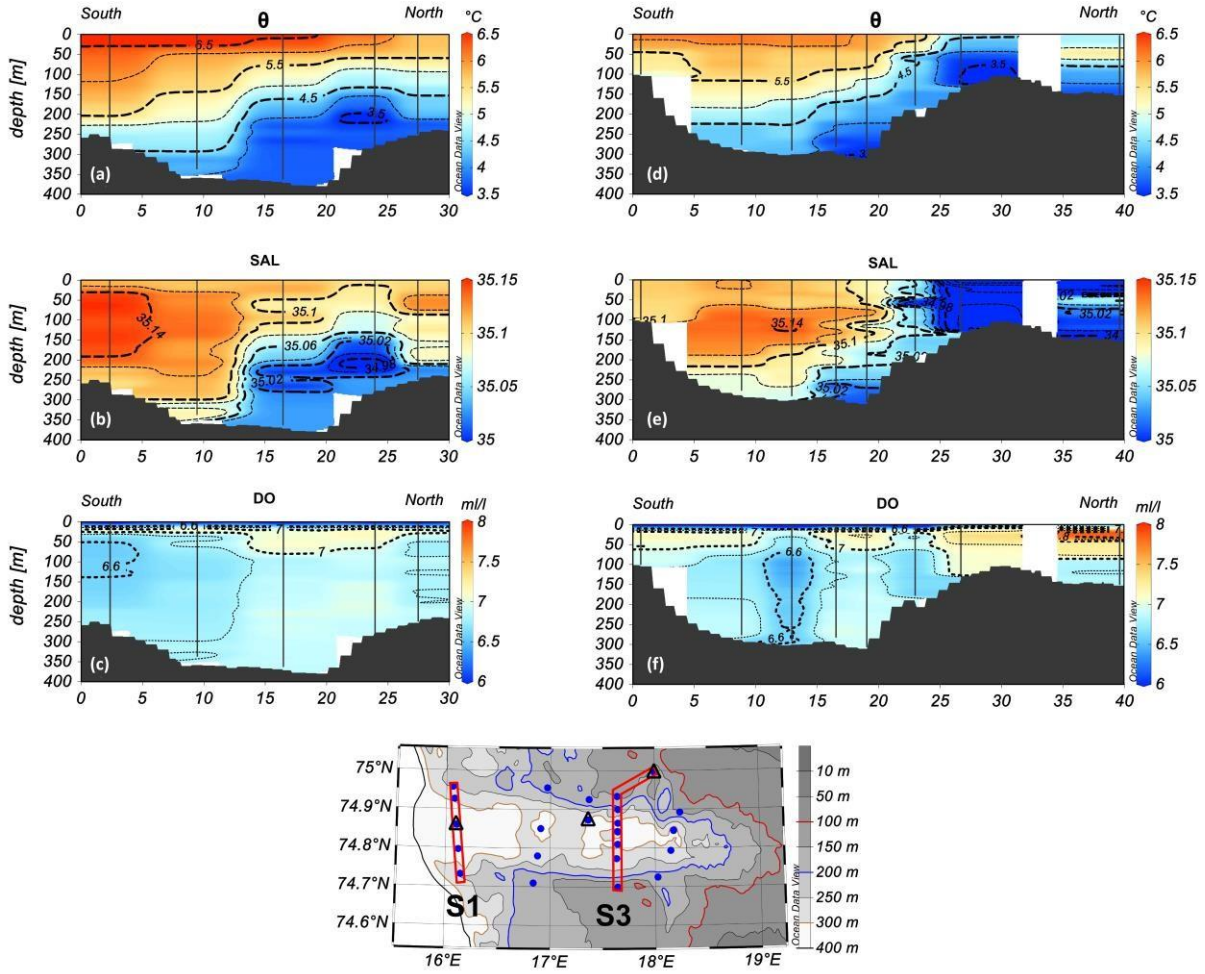

Fig. 2. Vertical distribution of potential temperature θ (°C), salinity (SAL) and dissolved oxygen DO (ml/l), along south- north sections S1 (a, b, c) and S3 (d, e, f). The blue filled circles in the sections S1 and S3 indicate the oceanographic stations, while triangles indicate the MUC stations.

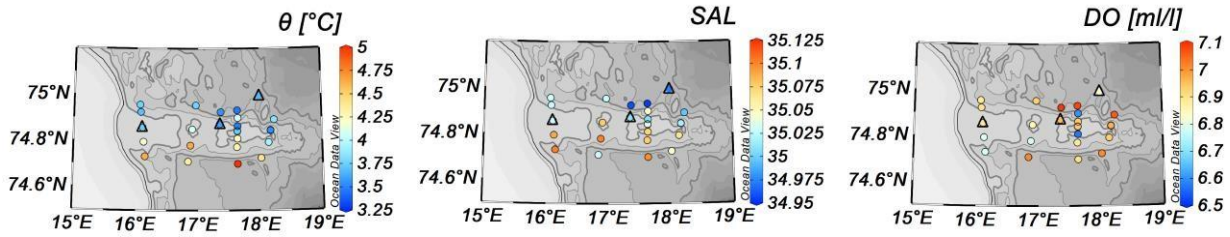

Fig. 3. Near bottom values of potential temperature θ (°C), salinity SAL, and dissolved oxygen DO (ml/l), from the CTD data. The triangles indicate the position of the MUC stations used in this work.

The current speed has been measured through most of the water column along the ship's route (Fig. 4a), and it vary between nearly 0 and 0.4 m/s (Fig. 4b). Highest values are recorded between 150 and 200 m water depth near the western border of the Kveithola Trough. Current speeds are low and not exceeding 0.09 m/s in the deeper parts of the water column, while high values are found over areas with the shallower depths within Kveithola.

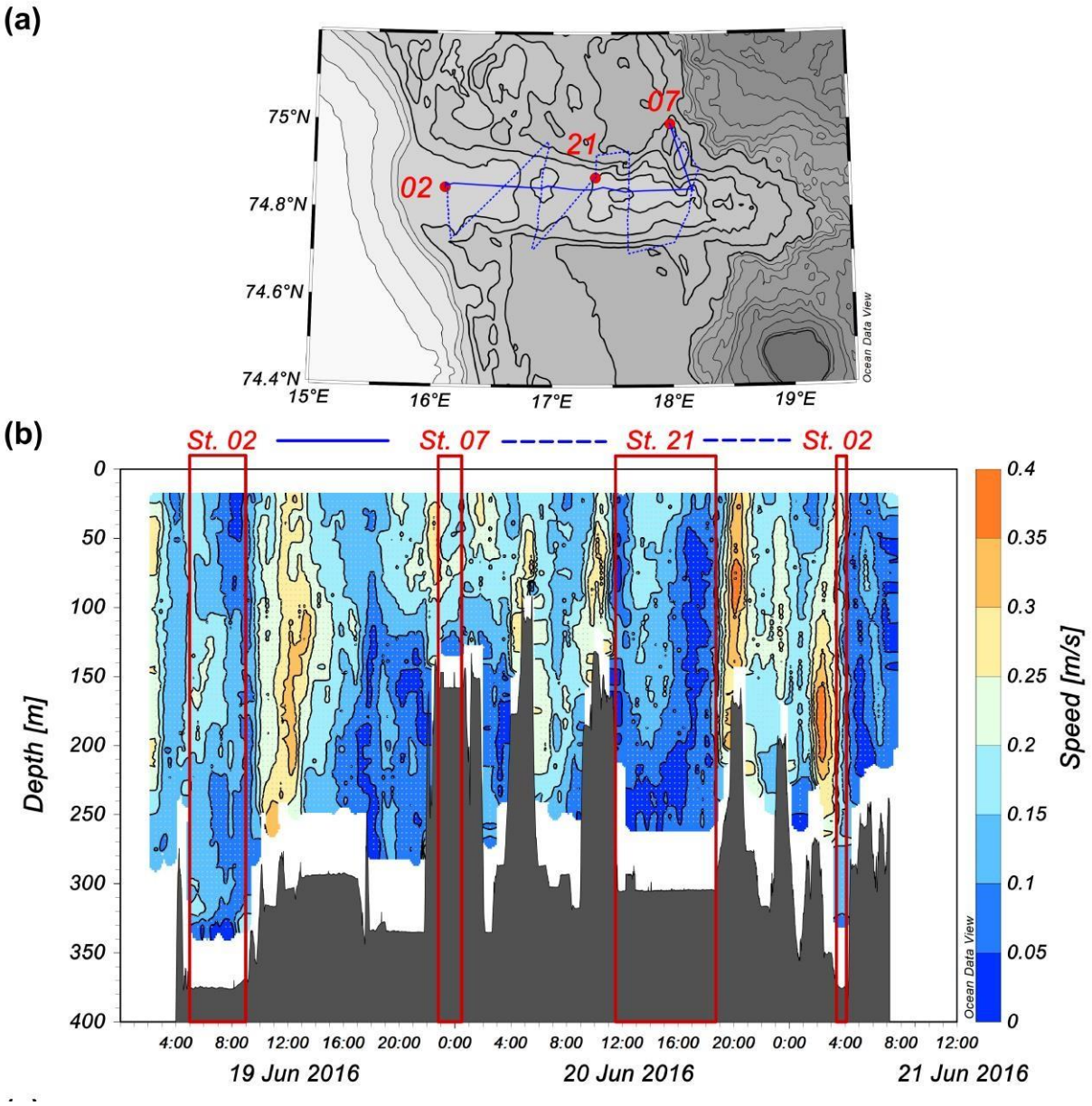

Fig. 4.Current speed the Kveithola Trough. (a) The red filled circles show the location of the three MUC stations (02, 07, and 21) and the track of the ship's route (blue solid line: from St. 02 to St. 07, blue dashed line: from St. 07 towards Sts. 21 and 02). (b) Time-depth diagram of current speed. Station 02 has been surveyed at the beginning and at the end of the cruise.

4.2 Sea ice extension

The maximum seasonal sea ice extent in the Barents Sea usually occurs between March and April. Winter 2016 has been characterised by the lowest sea ice extent during the last 40 years (NSIDC, https://nsidc.org/), and little sea ice has been observed in the study area (Fig. 5). In recent years, this area of the Arctic has often been characterised by the absence of ice during the winter period (e.g., Peng et al., 2018). One has to go back to winter 2013 to find sea ice throughout the north-western basin of the Barents Sea, even near the Kveithola Trough (Fig. 5), while the last above-average value for the period 1979-2019 has been recorded in 1998 and 2003.

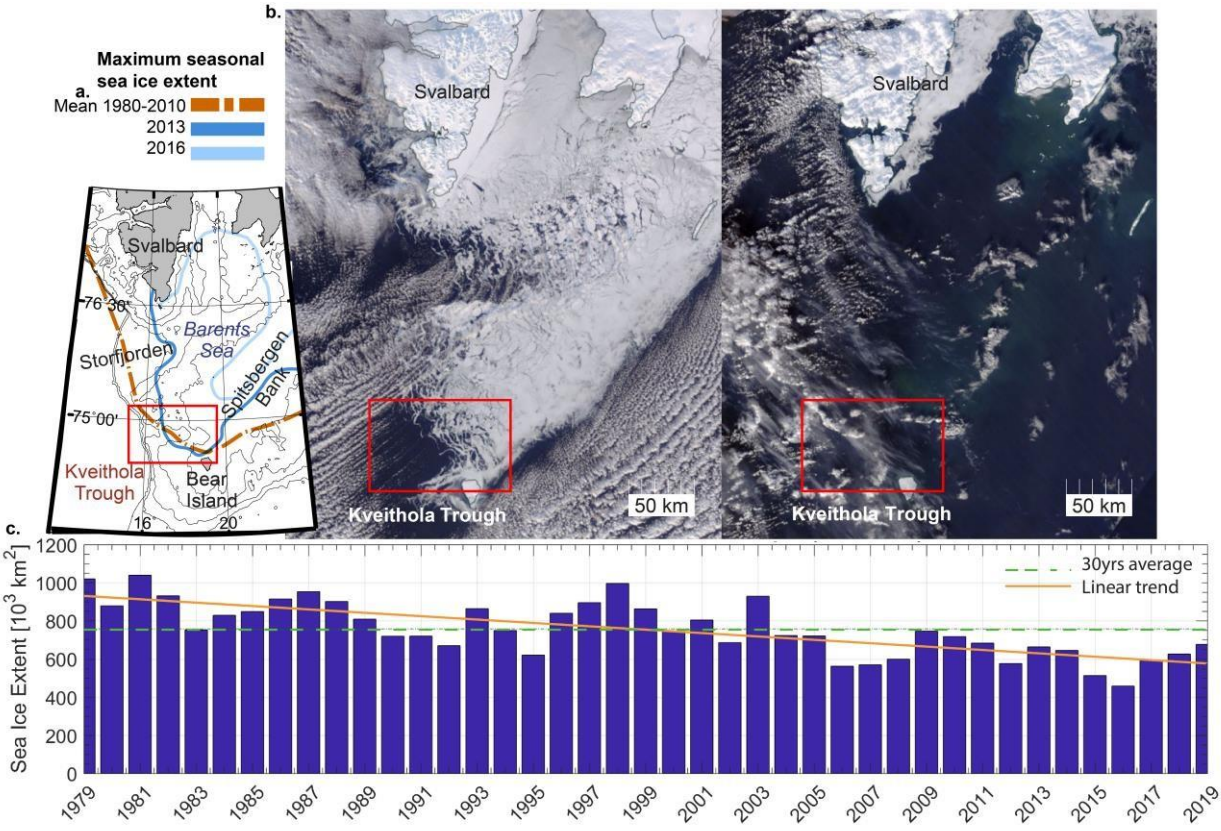

Fig. 5. (a) Map of the Barents Sea showing the average maximum seasonal sea ice extent during 1980-2010 (orange dashed line), in 2013 (dark-blue line), and in 2016 (light-blue line) (NSIDC,

https://nsidc.org/). (b) Satellite images (Terra/Modis, true-colour corrected reflectance) from 8 March 2013 (on the left) and 12 March 2016 (on the right) showing the maximum seasonal sea ice extent in the north-western Barents Sea (the Svalbard Archipelago and the Storfjorden are visible in the northern part of the images). (c) Time series of the mean monthly sea-ice extent in April in the Barents Sea, the month that normally has the largest sea-ice coverage in the area (Norwegian Polar Institute, www.mosj.no) for the period 1979 - 2019. The 30 years-average value (green dashed line) and the linear trend (yellow line) throughout the period are also indicated.

4.3 Grain size and sedimentation rate (SR)

The general grain size for the upper 10 cm of the multicore from station 02 is silt-fine sand (63-150 µm), coarse silt (31-63 µm) in station 21, and medium to coarse silt (8-15 µm -6 phi) in station 07 (Tab. 1).

Activity-depth profiles of excess ^{210}Pb show a quasi-exponential downcore decline, with only small fluctuations (supplementary material SF. 1).

Station 02, located in the Trough mouth, is characterised by the lowest average SR (on avg. 0.08 cm/yr). Stations 21 and 07 have higher sedimentation rates 0.13 and 0.22 cm/yr, respectively. ^{137}Cs activities are very low, often below the detection limit. However, at station 07, the Chernobyl peak of 1986 is recognizable, supporting SR values based on the ^{210}Pb profile. The obtained values of SR are comparable with those previously reported for the Barents Sea (e.g., Zaborska et al., 2008). Based on calculated SRs, the analysed sedimentary intervals span from 115 years (station 02) to 43 (station 07) (supplementary material ST. 1).

4.4 General faunal distribution and diversity indexes

The analysis of the living benthic foraminifera (size fraction ≥150 µm) have identified 23 species, where 19 are calcareous and 4 species agglutinated. In general, the living foraminiferal assemblages are mainly composed by *ca.* 70-80% of calcareous taxa and 18-26% of agglutinated taxa (Fig. 6; Tab. 2). The highest number of living foraminiferal individuals is found at station 07 with 149 individuals. Yet, station 02 show a more diverse fauna with 15 species. For all the stations, the highest concentration of living foraminifera is found in the first 2- 3 cm bsf. The maximum concentration is registered at station 07 with 5 spec./g at 2 cm bsf. At this station, the living foraminifera are also found down to the maximum depth of 9 cm bsf (Fig. 7). Generally, the dominance value (D) increases to 1 cm down core indicating the predominance of a few or only one species. Station 02 show a high diversity of the living assemblage with a total D value of 0.1 (Tab. 2). Shannon (H) values decreases to 0 when depth increases, and only one taxon is present.

In the dead foraminiferal assemblages (fraction ≥150 µm), 68 benthic foraminiferal species (50 calcareous and 18 agglutinated) are identified. The distribution of the dead foraminiferal assemblage in the topmost 10 cm of sediment show a dominance of the calcareous species, which constitutes more than 95% in all the stations. The agglutinated species are present with a maximum of 2% at station 07. The number of taxa (S) ranges between 36 (station 21) and 49 (station 02). The concentration is 160 to 4977 spec./g, of which the major contributor is the calcareous group (see supplementary material ST. 2). For all the stations D values are relatively low (0.1 to 0.2 max.), indicating the equal presence of all the species in the assemblage. These values are in agreement with the high H values indicating many taxa with a few individuals in the assemblage. The calcareous benthic foraminifera are present in the entire record in all the stations, while the agglutinated foraminifera occur sporadically (see supplementary material ST 2 and 3).

Tab. 2: Foraminiferal concentrations and diversity data for each core in the size fraction ≥150 µm. Number of counted specimens (N), number of species (S), number of foraminiferal specimens per gram of sediment (spec./g), Dominance (D) and Shannon index (H). The total values are also indicated in bold font. See supplementary material ST. 2 and ST. 3 for the separate values for the calcareous and agglutinated groups.

Station	Core depth (cm) bsf	Living foraminiferal assemblages					Dead foraminiferal assemblages				
		N	S	spec./g	D	H	N	S	spec./g	D	H
02	0-0.5	25	8	3	0.2	1.9	403	29	3094	0.1	2.3
	0.5-1	15	8	2	0.2	1.9	337	30	3280	0.1	2.5
	1-1.5	2	2	0.2	0.5	0.7	302	28	2262	0.1	2.5
	1.5-2	4	2	0.4	0.5	0.7	342	27	4661	0.1	2.4
	2-3	3	2	0.2	0.6	0.6	313	26	4977	0.1	2.5
	3-4	-	-	-	-	-	420	26	3313	0.1	2.4
	4-5	2	2	0.1	0.5	0.7	315	29	4161	0.1	2.6
	5-6	-	-	-	-	-	286	27	3272	0.1	2.4
	6-7	2	2	0.1	0.5	0.7	368	25	4187	0.1	2.5
	7-8	-	-	-	-	-	310	21	2477	0.1	2.4
	8-9	-	-	-	-	-	363	23	1509	0.2	2.2
	9-10	-	-	-	-	-	325	22	2424	0.2	2.1
	0-10 (total)	**52**	**15**	**0.3**	**0.1**	**2.4**	**4084**	**49**	**3357**	**0.1**	**2.5**
21	0-0.5	7	3	1	0.6	0.8	302	25	4069	0.1	2.7
	0.5-1	29	6	4	0.4	1.2	373	29	3478	0.1	2.6
	1-1.5	10	3	1	0.7	0.6	351	22	3431	0.1	2.3
	1.5-2	6	3	1	0.4	1.0	585	24	4709	0.1	2.5
	2-3	-	-	-	-	-	339	23	2921	0.1	2.3
	3-4	1	1	0.1	1.0	0.0	418	22	2556	0.1	2.3
	4-5	-	-	-	-	-	386	26	2664	0.1	2.4
	5-6	-	-	-	-	-	425	20	4135	0.1	2.3
	6-7	-	-	-	-	-	524	22	8960	0.1	2.3
	7-8	-	-	-	-	-	567	20	6998	0.1	2.4
	0-8 (total)	**53**	**8**	**0.5**	**0.4**	**1.3**	**4270**	**36**	**4944**	**0.1**	**2.4**
07	0-0.5	22	9	2	0.2	2.0	377	38	160	0.1	2.9
	0.5-1	11	3	1	0.5	0.9	303	29	184	0.1	2.8
	1-1.5	11	3	1	0.4	0.9	296	26	165	0.1	2.8
	1.5-2	43	5	5	0.5	0.8	376	32	191	0.1	2.8
	2-3	28	4	2	0.4	1.1	318	30	232	0.1	2.6
	3-4	17	3	1	0.7	0.6	340	30	130	0.1	2.7
	4-5	6	3	0.3	0.4	1.0	247	29	302	0.1	2.7
	5-6	5	3	0.3	0.4	1.1	355	29	192	0.1	2.7
	6-7	4	2	0.2	0.6	0.6	322	28	222	0.1	2.8
	7-8	3	1	0.2	1.0	0.0	334	25	187	0.1	2.7
	8-9	1	1	0.1	1.0	0.0	321	27	205	0.1	2.6
	9-10	-	-	-	-	-	339	25	318	0.1	2.6
	0-10 (total)	**149**	**12**	**0.85**	**0.3**	**1.6**	**3928**	**48**	**214**	**0.1**	**2.8**

Fig. 6. Cumulative abundance (%) for foraminiferal test of different composition in the living and dead assemblage at each station: calcareous (calcareous perforate), miliolids (calcareous imperforate) and agglutinated. Note that the vertical axis starts at 50%.

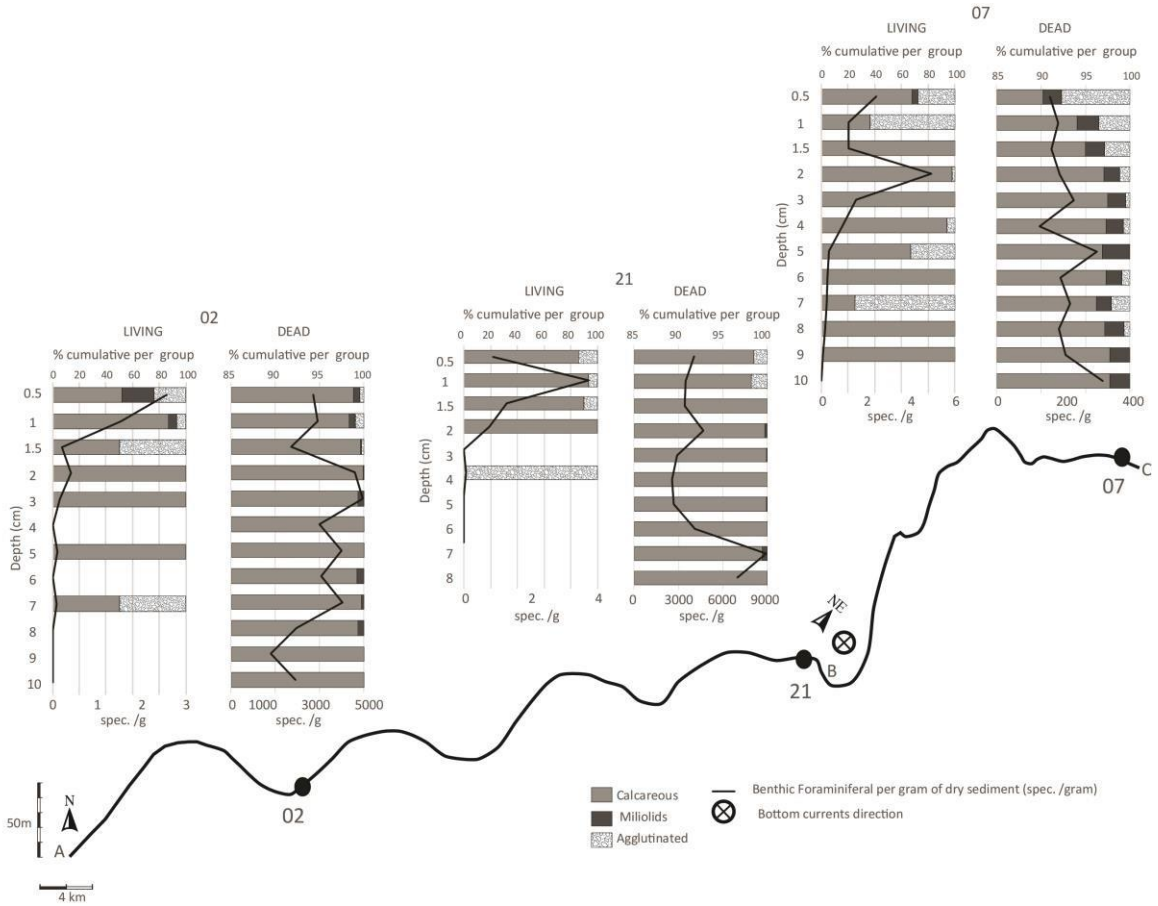

Fig. 7. Downcore living and dead foraminiferal concentrations, and distribution of calcareous (calcareous perforate), miliolids (calcareous imperforate), and agglutinated foraminifera shown along the bathymetric profile of Kveithola Trough. The location of the profile and the way points (A, B, C) are shown in Fig. 1. The black filled circles on the profile are the core locations. Note that the horizontal axis starts at 85% for the dead foraminifera.

4.5 Main foraminiferal species

The main calcareous living foraminiferal species are *Cassidulina neoteretis*, *Cibicidoides lobatulus*, *Globobulimina auriculata*, *Islandiella* spp., *Melonis barleeanus*, *Nonionella iridea*, *Nonionellina labradorica*, *Pullenia bulloide*s and *Trifarina angulosa* (Fig. 8 and 9; Plate 1). In our study, *T. angulosa* and *P. bulloides* exhibits an epifaunal microhabitat. Few individuals of *P. bulloides* and *C. lobatulus* are also found at 6-7 cm bsf (or deeper), probably transported by the bioturbation process. *C. neoteretis*, *Melonis barleeanus*, *N. labradorica, N. iridea* and *Islandiella* spp. show an infaunal habitat. *Globobulimina auriculata* is present in the first upper centimetres of sediment at station 21 and deeper at station 07.

The main dead foraminiferal species include only calcareous species as *Astrononion gallowayi*, *Buccella* spp., *Cassidulina laevigata*, *Cassidulina reniforme*, *C. neoteretis*, *C. lobatulus*, *Elphidium clavatum*, *Globocassidulina subglobosa*, *Islandiella* spp., *M. barleeanus*, *N. labradorica*, Rotaliida spp. and *T. angulosa* (Fig. 8 and 9; Plate 1).

The agglutinated foraminifera show high percentages (*ca.* 20-25%; Fig. 6) in the living foraminiferal assemblages. In all the stations, they are mainly represented by *Reophax* spp. including *Reophax scorpiurus* and *Reophax fusiformis*. In the dead foraminiferal assemblages, the agglutinated species occur with less than 2%, and only in stations 02 and 07. The main agglutinated species group is *Reophax* spp. Only few of the specimens are well preserved, whereas most *Reophax* spp. are partially or totally broken (Fig. 6; Plate 2).

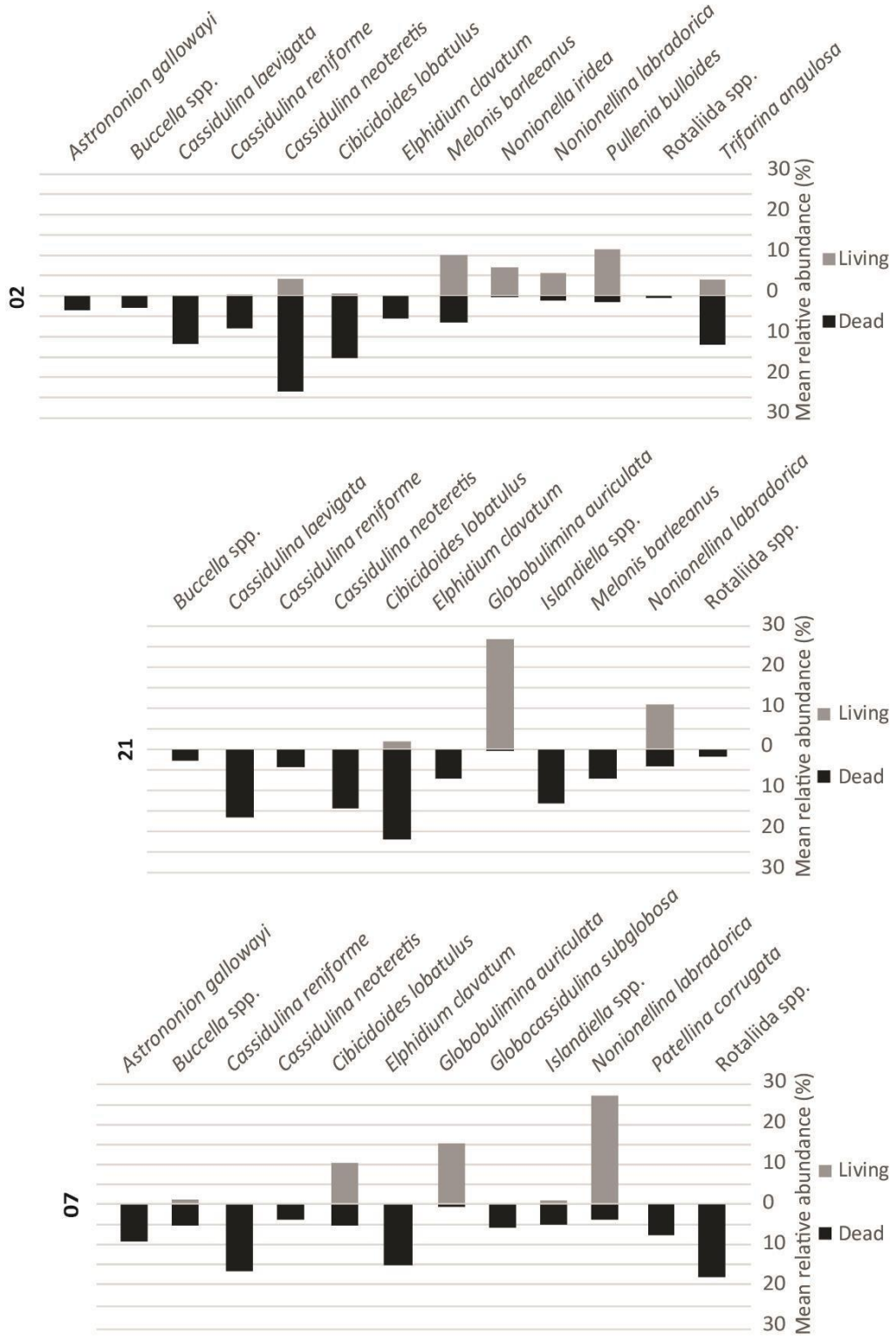

Fig. 8. Mean relative abundance of the main living and dead foraminiferal species, within the upper 0-10 cm of the studied cores.

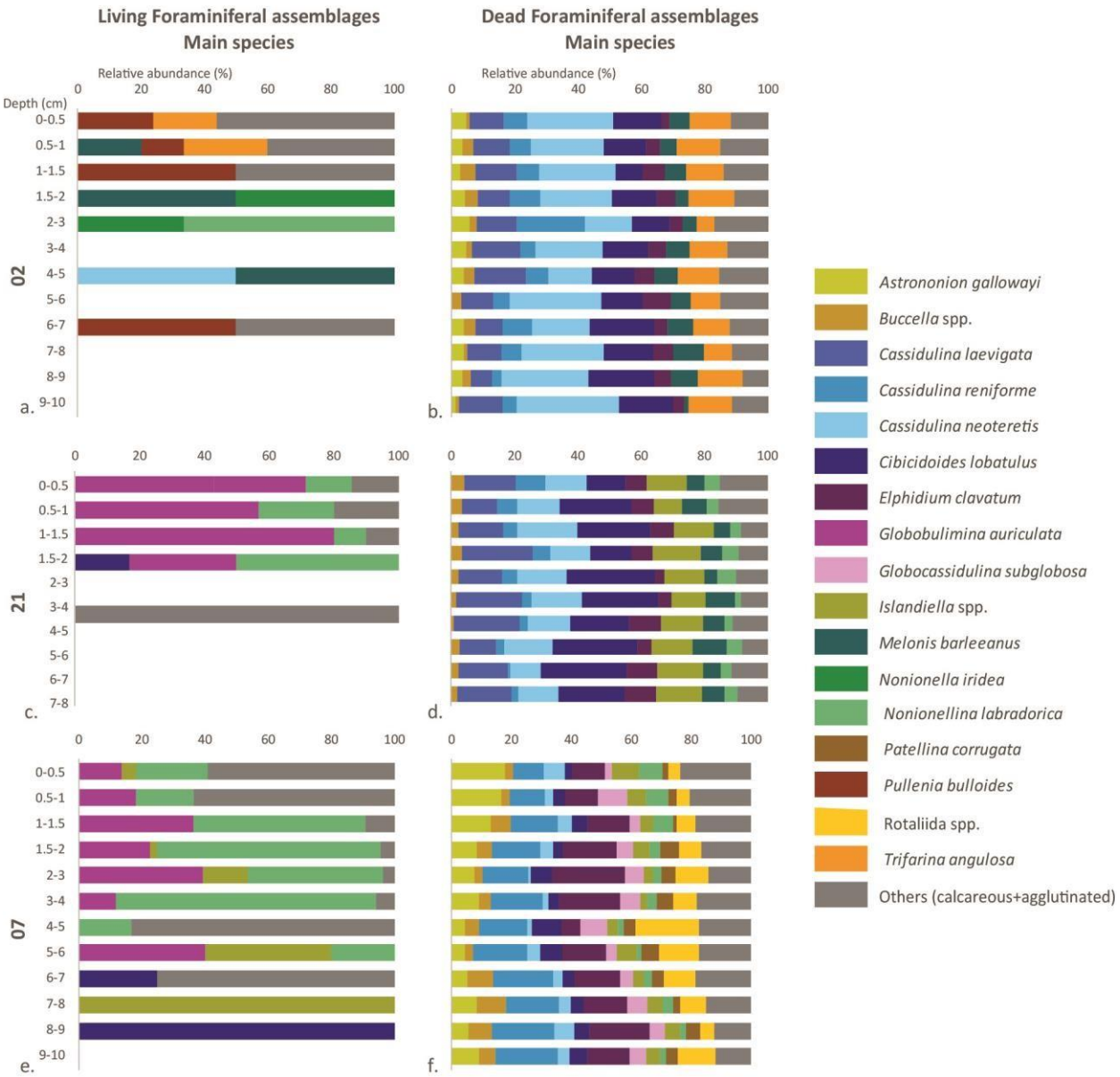

Fig. 9. Down core relative abundance of the main living and dead foraminiferal species.

The l/(l+d) ratios have been calculated for the main living and dead foraminiferal species (Tab. 3). The species *N. iridea* and *N. labradorica* are main contributors to the living foraminiferal assemblage at the three stations, whereas, for the dead foraminiferal assemblage, the abundance of the species vary throughout the trough. At station 02, the living species *M. barleeanus, N. iridea*, *N. labradorica* and *P. bulloides* are the most abundant species, whereas *C. reniforme*, *C. neoteretis*, *C. lobatulus* and *T. angulosa* are most frequent in the dead assemblage. At station 21 *G. auriculata*, *N. iridea*, *N. labradorica* are more abundant in the living assemblage than in the dead assemblage. In the dead assemblage at the station 21, the most abundant species are *C. lobatulus* and *P. bulloides*. At station 07, the most frequent living species are *C. lobatulus*, *G. auriculata*, *N. iridea* and *N. labradorica*, while it changes in the dead assemblage to *Buccella* spp. and *M. barleeanus*.

Tab. 3: Relative abundance of the main foraminiferal species in the living and dead assemblages, and the relative contribution of the main living species (l/(l+d). The black boxes show the higher relative contribution of the living foraminiferal fauna (0.4 to 1.00). The grey boxes show the higher relative contribution of the dead foraminiferal fauna (0.01 to 0.39). Main species that were only present in the dead or living assemblages are also listed. Note *N. iridea* and *P. bulloides* were only main species at the station 02 in the living assemblage; however, their values in other stations are shown.

%	**02**			**21**			**07**		
Main Species	LIVING (l)	DEAD (d)	l/(l+d)	LIVING (l)	DEAD (d)	l/(l+d)	LIVING (l)	DEAD (d)	l/(l+d)
Astrononion gallowayi	0	3.31	0	0	1.95	0	0	9.21	0
***Buccella* spp.**	0	2.76	0	0	2.50	0	1.14	5.24	0.18
Cassidulina laevigata	0	11.59	0	0	16.33	0	0	1.27	0
***Cassidulina* reniforme**	0.33	7.76	0.04	0	4.11	0	0	16.62	0
Cassidulina neoteretis	4.17	23.31	0.15	0	14.04	0	0	3.81	0
Cibicidoides lobatulus	0.56	14.89	0.04	1.85	21.72	0.08	10.42	5.18	0.67
Elphidium clavatum	0	5.30	0	0	6.92	0	0	15.24	0
Globobulimina auriculata	0	0.03	0	27.00	0.20	0.99	15.16	0.67	0.96
Globocassidulina subglobosa	0	0.42	0	0	1.30	0	0	5.73	0
***Islandiella* spp.**	0	0.58	0	0	12.89	0	0.38	4.97	0.07
Melonis barleeanus	10.00	6.32	0.61	0	6.84	0	0	0.43	0
Nonionella iridea	6.94	0.04	0.99	0.74	0	1.00	0.38	0	1.00
Nonionellina labradorica	5.56	0.85	0.87	10.85	4.00	0.73	27.32	3.71	0.88
Patellina corrugata	0	0.18	0	0	0.10	0	0	3.93	0
Pullenia bulloides	11.44	1.32	0.90	0.70	4.02	0.15	0	0.47	0
Rotaliida spp.	0	0.14	0	0	0.84	0	0	9.32	0
Trifarina angulosa	3.89	11.85	0.25	0	0.17	0	0	0.08	0

5. Discussion

5.1 Living foraminiferal assemblages and modern oceanographic conditions.

The distribution of foraminiferal fauna sampled in 2016 along the Kveithola transect reveal a strong variability in the seabed conditions, water column characteristics, and trophic status along the trough and on the shelf.

Station 02, in the outer trough, is strongly dominated by Atlantic water throughout the water column at the moment of the sediment sampling, which probably caused relatively high density and diversity of the living foraminiferal assemblage (Tab. 2). The living foraminiferal assemblage is also dominated by *M. barleeanus*, which thrives within relatively warm Atlantic water (Tab. 4). The vertical distribution of the living foraminiferal fauna is limited to 6- 7 cm bsf (Figs. 7 and 9) and dominated by the detritivore *M. barleeanus*, *P. bulloides* and *T. angulosa*. The living faunal distribution may indicate oligotrophic conditions (Tab. 4), and the bioavailable carbon value (BAC) is low at this station (Tab. 1). This is consistent with a limited supply of nutrition caused by less sea ice in the core site in the winter 2016, hence resulting in reduced seasonal algal blooms (Sakshaug and Slagstad, 1992; Wassmann et al., 1994) and less nutrition to the seabed.

At station 21, in the inner part of the trough, the bottom environment is characterised by different oceanographic conditions than station 02. Station 21 is more influenced by cold and less saline shelf waters. In addition, station 21 is influenced by intermittent seepage activity, where the accumulation of organic matter causes oxygen decrease within the sediment (Tab. 1). Here, the benthic assemblage is dominated by *G. auriculata* related to dysoxic environments and *N. labradorica*, which is typically associated with organic-rich sediments (Corliss, 1991; Koho et al., 2008) (Tab. 4). *N. labradorica* is a deep infaunal species that feeds mainly on the buried organic matter (Corliss, 1991). *Globobulimina* genus

usually lives in meso-eutrophic settings, deep in the sediments within or below the oxic-redox interface (e.g. Licari et al., 2003; Koho et al., 2008). These two taxa may become very abundant if rich sources of food are available, acting also as indicators of highly productive conditions (e.g., Jernas et al., 2018). Due to the intermittent seepage activity observed in the area (Lucchi et al., 2016; Bazzaro et al., 2020) and the presence of dysoxic indicators, we suppose the existence of a strong oxygen gradient at the water-sediment interface. *Nonionellina* and *Globobulimina* taxa are not considered endemic to seeps, nevertheless, they belong to genera that can respire nitrate instead of oxygen in environments where sulphurs are commonly present (Rathburn et al., 2003; Levin, 2005). This stressed environment could also cause the low faunal density and diversity (Tab. 2) and the vertical distribution of the living foraminiferal fauna, which is limited to the first 4 cm (Figs. 2, 3 and 9).

Station 07, in the north-eastern part of the study area, is mainly dominated by cold (<5°C) and less saline (<35) shelf waters. The core site is also influenced by sea ice in the winter 2016 (Fig. 5) and when seasonal sea ice melts during the spring primary productivity is enhanced (Sakshaug and Slagstad, 1992). These environmental conditions can explain the accumulation of organic matter driving the proliferation of abundant foraminiferal fauna, dominated by *Nonionella* spp. and *G. auricula*. The vertical distribution of benthic fauna down to 9 cm bsf (Tab. 1) may be related with the more oxygenated bottom waters, which favour the oxygen penetration into the sediments. Caridi et al. (2019) reported for the same station, a high macrofaunal bioturbation activity that can favour both the oxygen penetration and the mobility of the foraminifera in the first centimetres of the sediment.

5.2 Preservation and taphonomic processes

The living foraminiferal assemblages register a specific moment of environmental conditions, which improves our understanding of the environmental ranges of the observed species. The dead foraminiferal assemblages correspond to an average of the environmental conditions over time interval, which may record several years of deposition in a specific area. This improves our understanding of the dynamics of foraminiferal assemblages over the time. Therefore, in our study, the living foraminiferal assemblages gave an observation of the environmental conditions during the summer (June) 2016, while the dead foraminiferal assemblages showed the changes occurring over a larger temporal interval, giving an average of environmental conditions throughout several years (including all seasons).

The living foraminiferal assemblages can appear different from the dead foraminiferal assemblages leading to a correlation of different environmental conditions (Murray and Alve, 1999). The taphonomic processes, e.g. dissolution and desegregation, damage the foraminiferal test contributing to differences between living and dead foraminiferal assemblages.

In our stations, the main difference between living and dead assemblages is the preservation of the agglutinated species (Figs. 6 and 7). The occurrence of agglutinated foraminifera is partially or totally subordinated to that of calcareous species in both the living and dead assemblages due to major preservational problems (Fig. 6). Agglutinated foraminifera have a poor preservation potential due to the mechanical disaggregation, test compaction and degradation of the organic cement that binds together the agglutinated grains (Schröder, 1988; Murray, 2006). Furthermore, also the calcareous or iron compounds of agglutinates cement may dissolve or oxidize (De Stigter et al., 1999; Duros et al., 2014; Dessandier et al., 2018). Our results show an increase of broken agglutinated test below the first centimetres of sediments (Fig. 6), and the disappearance of the agglutinated taxa deeper in the sediment

(Fig. 7), both in oxygenated and dysoxic environments. Some studies (e.g., Schröder, 1988; De Stigter et al., 1999) have already pointed to this taphonomic process in different oceanographic contexts, estimated the loss of the dead agglutinated taxa of about 20% compared to the living species.

The calcareous foraminiferal tests suffer different mechanisms that can lead to their partial or total destruction (Murray, 2006). The dissolution affects especially the delicate and/or aragonitic calcareous tests. Species with delicate tests, such as *G. auriculata* (Ellis and Messina, 1940-1978), is very frequent in the living foraminiferal assemblages (Tab. 3; Fig. 8 and 9), yet its frequency is reduced in the dead foraminiferal assemblages, and many broken specimens have been observed (Plate 2). In this study, we have also frequently observed specimens of *Nonionellina labradorica* and *Nonionella iridea* having a broken ultimate chamber (Tab. 3; Figs. 8 and 9, Plate 2). The calcareous species also showed marks of predation like different boring patterns, holes and cavities that may be produced by phototrophic (cyanobacteria, chlorophyta) and heterotrophic (fungi) organisms (Cherchi et al., 2012). This predation weakens the test facilitating or producing the mechanical disaggregation of the test (Plate 2). In all these cases, the species are classified as detailed as possible especially in the cases when the fragment included the proloculus and/or the aperture zone, for which a correct classification could be made.

Post-mortem bioturbation and reworking of the sediments may also have caused fragmentation, corrosion and disintegration of the foraminiferal tests (Schröder, 1988; De Stigter et al., 1999; Loubere et al., 2011; Duros et al., 2014; Dessandier et al., 2018). These processes intensified with the increase of the amount of macrofauna, as described in Caridi et al. (2019). Bioturbation would facilitate the decrease or even the disappearance of some taxa from the dead foraminiferal record, especially for those specimens having delicate tests that are weaker or not well cemented (Tab. 3; Figs. 6 and 8; Plate 2).

In general, most calcareous specimens are found in good condition; hence, we are confident of suitability and quality of the foraminiferal record for paleoenvironmental reconstructions. The comparisons

between living and dead foraminiferal concentration (spec./g, Tab. 3) suggest a good preservation of most of the species. The dead foraminiferal assemblages include all the living foraminiferal species although occurring with different percentages. When comparing it should be taken into account that living foraminiferal assemblages represent specific environmental conditions while the dead foraminiferal assemblages represent a larger time interval and an average of yearly environmental characteristics. However, the current good agreement between assemblages indicate that the dead foraminiferal assemblages are robust paleoenvironmental indicators.

5.3 Paleoenvironmental variations during the last decades

The sedimentary records used for this study cover the last *ca.* 50-100 years (supplementary material ST. 1). The composition of the benthic foraminiferal assemblages in all three paleorecords is relatively stable, suggesting relatively stable environmental conditions during the investigated time interval.

The paleorecord from the outer trough, station 02 covers the last 115 years and is characterised by sandy sediments (Tab. 1). This suggests relatively strong bottom currents, which is also reflected by *C. lobatulus* that is often associated with higher dynamic environments (Fig. 4; Tab. 4). These high-energy conditions provided a constant supply of organic matter and oxygen, which probably increased the diversity of the assemblage (Tab. 2). Furthermore, the presence of *C. reniforme*, and *C. neoteretis*, with the warm-water indicator *C. laevigata* suggest a relatively strong influence by warm AW (Fig. 9). The foraminiferal record also show some influence of colder waters and sea ice at the station 02 during the last decades. At 2- 3 cm bsf (*ca.* 1986), both the frequency of cold-water species *C. reniforme* (Fig. 9) and the sea ice data increase (Fig. 5).

During the last ca. 64 years, the inner trough station (21), has recorded relatively stable environmental conditions. The presence of *Islandiella* spp. and *N. labradorica* indicate relatively higher trophic level.

Mesotrophic to eutrophic conditions could be related to the position of the core site close to the sea ice margin where high biological productivity can facilitate an accumulation of organic matter to the bottom (Tab. 2 and. 4; Fig. 9). The increased abundance of *Islandiella* spp., compared to station 02, indicates an increase of nutrients, probably related to a stronger influence of the marginal sea ice zone (Fig. 5). The foraminiferal assemblage also contains *C. laevigata*, *C. neoteretis* and *C. reniforme*, similar to station 02; reflecting comparable water masses conditions, with influence of both the relatively warm (AW) and cold water masses.

The record from the shelf area (station 07), which covers the last *ca.* 43 years, is characterised by fresher and colder waters, in accordance with its northernmost position, and therefore, the greater influence of the Arctic water origin and longer periods of sea ice cover. The colder conditions are shown by the predominance of cold-water species *E. clavatum* and *C. reniforme* (Tab. 4). The decrease of species indicative of warmer conditions, *Buccella* spp., *Islandiella* spp., *N. labradorica* and *Melonis barleeanus*, show less influence of warm AW and the reduction in the quantity or quality of nutrients availability compared to the other stations (Fig. 8; Tab. 4).

Previous studies have shown how dead benthic foraminiferal assemblages have changed within the last two centuries in the SW and the central Barents Sea, reflecting a warming trend of the Atlantic water (Wilson et al., 2011; Dijkstra et al., 2017a). However, these progressively warming conditions are not observed in our record from Kveithola Trough possibly due to the extent of the current records (maximum *ca.* 100 years), comprising the already advancing warm period. Saher et al. (2012) observe a change to a dominance of warm water species between 1965-1992 and 2005-2005, which is probably related to the changed position of the ice edge in the central Barents Sea during this time interval. We also speculate the Kveithola Trough may have morphological features making it a more protected system as indicated by the oceanographic data collected during the cruise.

Tab. 4. Ecological characteristics of the main living and dead species.

MAIN SPECIES	ENVIRONMENTAL CONDITIONS	REFERENCES
Astrononion gallowayi	Temperature tolerant, epifaunal	Saher et al., 2009; Saher et al., 2012.
***Buccella* spp.**	Cold water, infaunal, often related to oceanic fronts/sea ice edges	Steinsund, 1994; Hald and Korsun, 1997; Saher et al., 2009; Saher et al., 2012.
Cassidulina laevigata	Warm water, infaunal	Sejrup et al., 2004; Saher et al., 2009; Steinsund, 1994; Dijikstra et al., 2017b.
Cassidulina reniforme	Cold water, infaunal	Hald and Korsun, 1997; Korsun and Hald, 1998; Murray, 2006; Saher et al., 2009; Saher et al., 2012; Dijikstra et al., 2017b.
Cassidulina neoteretis	Cold water, infaunal, associated with cooled Atlantic Water in the Barents Sea, prefers fresh phytodetritus	Saher et al., 2009; Seidenkrantz, 1995; Dijikstra et al., 2017b.
Cibicidoides lobatulus	Temperature tolerant, epifaunal, tolerates high energy environments	Steisund, 1994; Hald and Steisund, 1996; Wollenburg and Mackensen, 1998; Murray, 2006; Saher et al., 2009; Saher et al., 2012.
Elphidium clavatum	Cold water, infaunal, tolerates less than marine salinity	Steinsund, 1994; Sejrup et al., 2004; Murray, 2006; Saher et al., 2009; Saher et al., 2012; Dijkstra et al., 2017b.
Globobulimina auriculata	Temperature tolerant, infaunal, facultative anaerobe, tolerates dysoxia, detritivore	Gooday et al., 2001; Murray, 2006; Murray and Alve, 2016.
Globocassidulina subglobosa	Cold water, infaunal, low organic content, infaunal, detritivore	Murray, 2006.
***Islandiella* spp.**	Cold water, infaunal, free, detritivore, high availability of nutrition	Steinsund, 1994; Murray, 2006; Saher et al., 2009; Saher et al., 2012; Dijkstra et al., 2017b.
Melonis barleeanus	Relatively warm water, infaunal, tolerates dysoxia, detrivore, related to degraded organic matter	Steinsund, 1994; Murray, 2006; Saher et al., 2009; Saher et al., 2012; Dijkstra et al., 2017b.
Nonionella iridea	Cold water, infaunal, phytodetritus species, infaunal	Murray, 2006.
Nonionellina labradorica	Cold water, infaunal, associated with high availability of nutrition	Sejrup et al., 2004; Murray, 2006; Saher et al., 2009; Saher et al., 2012.
Patellina corrugata	Temperature tolerant, epifaunal, associated with high availability of nutrition	Murray, 2006
Pullenia bulloides	Temperature tolerant, infaunal, detrivore	Murray, 2006; Saher et al., 2009.
Trifarina angulosa	Temperature tolerant, epifaunal, tolerates high energy environments	Steinsund, 1994; Murray, 2006; Saher et al., 2009.

6. Conclusions

Geological and oceanographic data collected during the Eurofleets 2- BURSTER cruise in June 2016 reveal a highly dynamic marine environment in the Kveithola Trough.

The CTG-labelled living foraminiferal from the outer station (02) influenced by AW, show that the living foraminiferal assemblages are dominated by the warm water species *M. barleeanus* and the tolerant temperature species, *P. bulloides.* In the inner station 21, the living foraminiferal assemblages is dominated by the high food supply indicator *N. labradorica,* and by the dysoxia species, *G. auriculata* related to the presence of methane seepage. The shelf station (07) is dominanted are by *G. auriculata*, *N. labradorica* and the high-dynamic environmental indicator, *C. lobatulus*. The dominance of warmer water species in the outer shelf and the presence of eutrophic species in the inner part of the trough reflect the oceanographic conditions during the sampling period and the high availability of organic matter to the seafloor.

The taphonomical processes affect the preservation of the foraminiferal test, especially the agglutinated foraminifera, increasing the possibility of bias in the paleoenvironmental interpretation when using these taxa. We have found the preservation of most of the calcareous species is good, and they may contribute to robust paleoenvironmental records.

The dead foraminiferal assemblages show no significant changes during the last *ca.* 100 years. At station 02, the dead foraminiferal assemblages show the influence of relatively warm AW by *C. laevigata* and *C. neoteretis* and relatively strong hydrodynamic conditions by *C. lobatulus*. The paleoenvironmental record at station 21 shows similar conditions to the outer part of the trough. Yet the increased abundances of *Islandiella* spp. and *N. labradorica* indicate a higher trophic level probably reflecting an increased influence of seasonal sea ice and increased nutrient influx. The dominant species at station 07 are the

cold-water indicators *C. reniforme* and *E. clavatum*, mirroring to the northern position of this station with a larger influence of colder water and sea ice.

The dead foraminiferal assemblages in Kveithola Trough show no significant changes during the last *ca.* 100 years. In contrast to other studies from other areas of the Barents Sea that indicate a larger and progressively increasing influence of the Atlantic water either within the last 200 years (WIlson et al., 2011; Dijkstra et al., 2013) or with the last ca. 30 years (Saher et al., 2012). This may be due to the current study is shorter than the others are and it does not record pre-impacted conditions or the time interval being recorded yet. We also speculate that the local morphology of the Kveithola Trough may protect the environmental system from external influences responsible for the changes recorded in other parts of the Barents Sea.

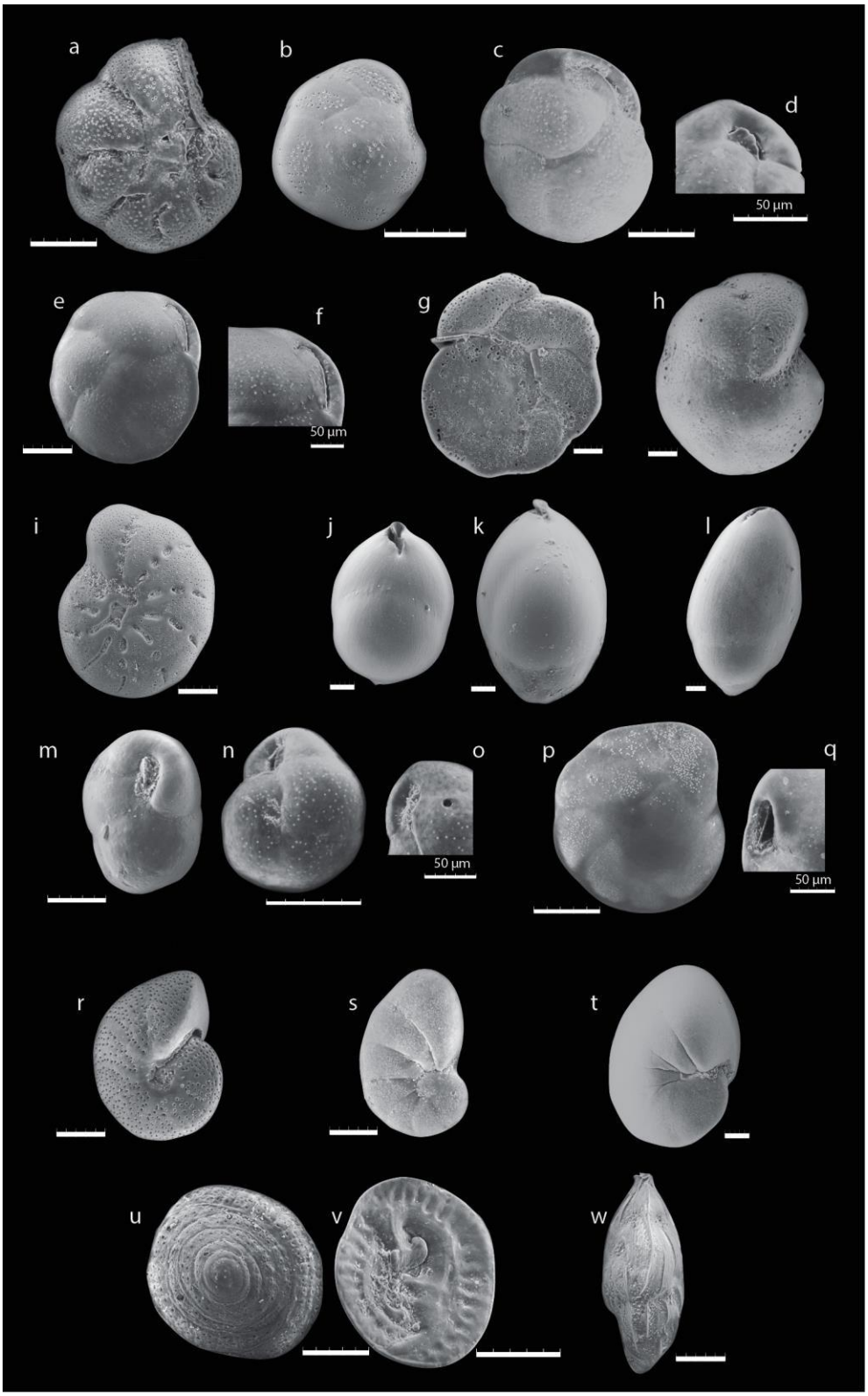
a
b
c
d
50 µm
e
f
50 µm
g
h
i
j
k
l
m
n
o
50 µm
p
q
50 µm
r
s
t
u
v
w

Plate 1: Some of the main calcareous dead foraminiferal species: (a) *Astrononion gallowayi*; (b) *Buccella* spp.; (c) *Cassidulina reniforme*, (d) *C. reniforme* zoom of the aperture; (e) *Cassidulina neoteretis*, (f) *C. neoteretis* zoom of the aperture; (g-h) *Cibicidoides lobatulus*; (i) *Elphidium clavatum*; (j- k- l) *Globobulimina auriculata;* (m-n) *Globocassidulina subglobosa;* (o) *G. subglobosa* zoom of the aperture; (p-q) *Islandiella* spp.; (r) *Melonis barleeanus*; (s) *Nonionella iridea*; (t) *Nonionellina labradorica*; (u) *Patellina corrugata*; and (w) *Trifarina angulosa.* Scale-bar 100 µm, except for the different measure indicated above the scale-bar.

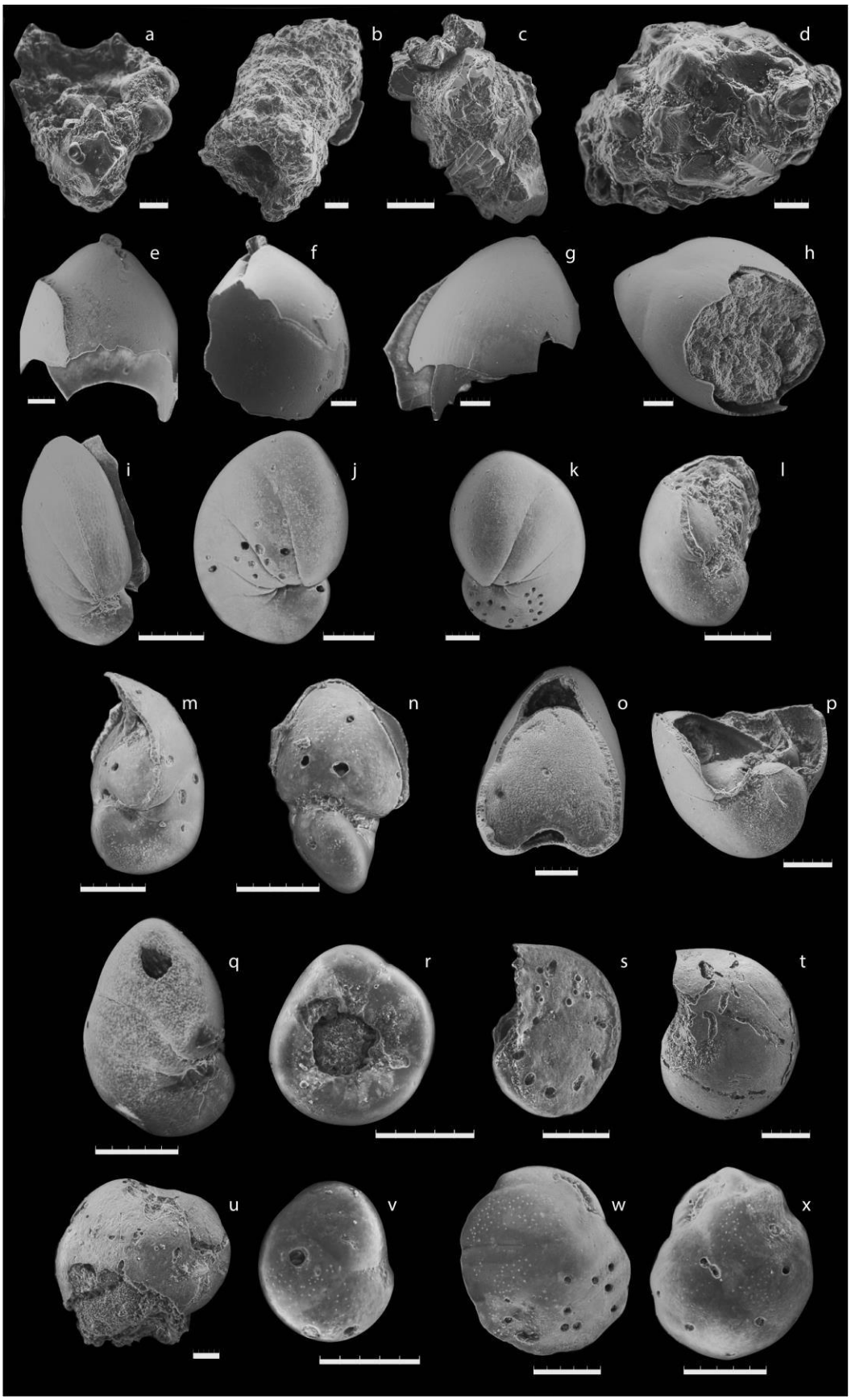
a
b
c
d
e
f
g
h
i
j
k
l
m
n
o
p
q
r
s
t
u
v
w
x

Plate 2: Dead foraminiferal species with taphonomic processes evidences: (a-d) Fragments of agglutinated foraminifera; (e-h) Fragments of *G. auriculata*; (i-q) *N. iridea* and *N. labradorica*: (i) broken test, (j-k) holes (marks predation?), (l-m-n) last chamber broken: (l) partially filled with sediment and (m-n) with holes (predation or post mortem activity?), (o) last chamber separate of the rest of the test, (p) total breakage of the last chambers, (q) last chamber broken (mechanically?); (r) Rotaliida indet. ventral broken; (s- t) *C. lobatulus*: (marks predation?): (s) holes, (t) cavities; (u) *Cassidulina* spp. with marks, broken and partially filled; (v) *C. reniforme* holes (marks predation?); and (w-x) *C. neoteretis* holes (marks predation?). Scale-bar 100 µm.

Acknowledgments

We would like to firstly acknowledge Eurofleets2 for the great support by funding the data acquisition of the project BURSTER (Bottom currents in a stagnant environment), on-board of the R/V Polarstern (expedition PS99-1). We also thank the Captain, crew and scientific party of exp. PS99-1 and Thomas Soltwedel for the important advice during the cruise preparation and the expedition. Thanks to Massimo Tagliaferro for the basics to the use of SEM during the cruise. Data analyses were funded by the PNRA project AXED (Anoxic environments in Arctic sediment drifts) through the University of Pisa (Italy). The University of Costa Rica is acknowledged for the PhD scholarship to Viviana Maria Gamboa Sojo. The acquired data from the vmADCP were processed after the cruise by Laura Ursella (OGS). Thanks to Karen Gariboldi and Diana Segura Sojo for their comments in the final stages of the writing process.

Author contributions

R.G.L. and **C.M.** conceived and designed the research. **R.G.L.** PI of BURSTER project. **C.M.** PI of AXED project and conceptualization. **V.M.G.S., F.C., A.S., R.G.L., M.B., V.K., A.T.D., P.P., C.M.** acquired data at sea during the BURSTER cruise. **V.M.G.S.** processed and analysed the dead foraminiferal assemblages and living data ≥150 µm. **V.M.**, **C.M.** and **K.H.** analysed the dead foraminiferal assemblages data. **F.C.** and **A.S.** processed and analysed the living foraminiferal assemblages. **R.G.L.** processed sedimentological data. **M.B., V.K.** processed and analysed oceanographic data. **A.T.D.** processed ^{210}Pb and ^{137}Cs radionuclide measurements. **L.L.** and **A.T.D.** calculated ^{210}Pb-based sedimentation rates**. P.P.** carried out grain size analysis. **V.M.G.S**. wrote the most of the manuscript with contributions from: **C.M.** and **K.H.** dead foraminiferal assemblages, preservation and taphonomic processes; **F.C.** and **A. S.** Living foraminiferal assemblages and modern situation; **R.G.L.** grain size and sedimentological analyses; **M.B.** and **V.K.** oceanographic data and water masses properties; **L.L.** and **A.T.D.** age model and sedimentation rate. All authors discussed the results, the conclusions and reviewed the manuscript.

References

Aagaard, K., 1989. A synthesis of the Arctic Ocean circulation. Le Conseil. Rapp. P. V. Reun. Cons. Int. Explor. Mer. 188, 11 – 22.

Aagaard, K., Coachman, L. K., Carmack, E., 1981. On the halocline of the Arctic Ocean. Deep Sea Research. Part A 286, 529-545.

Aagaard, K., Swift, J. H., Carmack, E. C., 1985. Thermohaline circulation in the Arctic Mediterranean seas. Journal of Geophysical Research. Oceans 90C3, 4833-4846.

Aagaard, K., Darnall, C., Greisman, P., 1973. Year-long current measurements in the Greenland-Spitsbergen passage. Deep Sea Research. 20 (8), 743-746.

Bazzaro, M., Ogrinc, N., Relitti, F., Lucchi, R.G., Giani, M., Adami, G., Pavoni, E., De Vittor, C., 2020. Geochemical signatures of intense episodic anaerobic oxidation of methane in near-surface sediments of a recently discovered cold seep (Kveithola trough, NW Barents Sea). Marine Geology, 425, 106189.

Bjarnadóttir, L. R., Rüther, D. C., Winsborrow, M. C., Andreassen, K., 2013. Grounding-line dynamics during the last deglaciation of Kveithola, W Barents Sea, as revealed by seabed geomorphology and shallow seismic stratigraphy. Boreas, 42(1), 84-107.

Bernhard, J. M., Ostermann, D. R., Williams, D. S., Blanks, J. K., 2006. Comparison of two methods to identify live benthic foraminifera: A test between Rose Bengal and CellTracker Green with implications for stable isotope paleoreconstructions. Paleoceanography 214.

Caridi, F., Sabbatini, A., Morigi, C., Dell'Anno, A., Negri, A., Lucchi, R.G., 2019. Patterns and environmental drivers of diversity and community composition of macrofauna in the Kveithola Trough NW Barents Sea. Journal of Sea Research 153, 101780.

Carpenter, J.H., 1965. The Chesapeake Bay Institute technique for the Winkler dissolved oxygen method. Limnology and Oceanography 101, 141-143.

Cherchi, A., Buosi, C., Zuddas, P., De Giudici, G.B., 2012. Bioerosion by microbial euendoliths in benthic foraminifera from heavy metal-polluted coastal environments of Portovesme south-western Sardinia, Italy. Biogeosciences 9, 4607–4620.

Comiso, J.C., Hall, D.K., 2014. Climate trends in the Arctic as observed from space. Wiley Interdisciplinary Reviews: Climate Change 53, 389-409.

Corliss, B.H., 1991. Morphology and microhabitat preferences of benthic foraminifera from the northwest Atlantic Ocean. Marine Micropaleontology. 173-4, 195-236.

De Stigter, H.C., Van der Zwaan, G.J., Langone, L., 1999. Differential rates of benthic foraminiferal test production in surface and subsurface sediment habitats in the southern Adriatic Sea. Palaeogeography, Palaeoclimatology, Palaeoecology. 1491-4, 67-88.

Dessandier, P.A., Bonnin, J., Kim, J.H., Racine, C., 2018. Comparison of living and dead benthic foraminifera on the Portuguese margin: Understanding the taphonomical processes. Marine Micropaleontology. 140, 1-16.

Dijkstra, N., Junttila, J., Carroll, J., Husum, K., Hald, M., Elvebakk, G., Godtliebsen, F., 2013. Baseline benthic foraminiferal assemblages and habitat conditions in a sub-Arctic region of increasing petroleum development. Marine environmental research, 92, 178-196.

Dijkstra, N., Junttila, J., Aagaard-Sørensen, S., 2017a. Environmental baselines and reconstruction of Atlantic Water inflow in Bjørnøyrenna, SW Barents Sea, since 1800 CE. Marine Environmental Research. 132, 117-131.

Dijkstra, N., Junttila, J., Skirbekk, K., Carroll, J., Husum, K., Hald, M., 2017b. Benthic foraminifera as bio-indicators of chemical and physical stressors in Hammerfest harbor Northern Norway. Marine pollution bulletin, 1141, 384-396.

Dowdeswell, J.A., Fugelli, E.M.G., 2012. The seismic architecture and geometry of grounding-zone wedges formed at the marine margins of past ice sheets. GSA Bulletin 12411-12, 1750-1761.

Duplessy, J.C., Ivanova, E., Murdmaa, I., Paterne, M., Labeyrie, L., 2001. Holocene paleoceanography of the northern Barents Sea and variations of the northward heat transport by the Atlantic Ocean. Boreas 301, 2-16.

Duros, P., Fontanier, C., De Stigter, H. C., Cesbron, F., Metzger, E., Jorissen, F. J., 2012. Live and dead benthic foraminiferal faunas from Whittard Canyon (NE Atlantic): Focus on taphonomic processes and paleo-environmental applications. Marine Micropaleontology, 94, 25-44.

Duros, P., Jorissen, F.J., Cesbron, F., Zaragosi, S., Schmidt, S., Metzger, E., Fontanier, C., 2014. Benthic foraminiferal thanatocoenoses from the Cap-Ferret Canyon area NE Atlantic: a complex interplay between hydro-sedimentary and biological processes. Deep Sea Research. Part II 104, 145-163.

Ellis, B.E., Messina, A.R., 1940–1978. Catalogue of Foraminifera. Micropaleontology Press, Am. Museum of Natural History, New York.

Feyling-Hanssen, R.W., Jørgensen, J.A., Knudsen, K.L., Lykke-Andersen, A.L., 1971. Late Quaternary Foraminifera from Vendsyssel, Denmark and Sandnes, Norway. Geological Society of Denmark 21, 67-317.

Fohrmann, H., Backhaus, J.O., Blaume, F., Rumohr, J., 1998. Sediments in bottom-arrested gravity plumes: Numerical case studies. Journal of Physical Oceanography. 2811, 2250-2274.

Friedman, G.M., Sanders, J.E., 1978. Principles of sedimentology. Wiley, New York.

Gooday, A. J., Hughes, J. A., Levin, L. A., 2001. The foraminiferan macrofauna from three North Carolina (USA) slope sites with contrasting carbon flux: a comparison with the metazoan macrofauna. Deep Sea Research Part I: Oceanographic Research Papers, 48(7), 1709-1739.

Green, K.E., 1960. Ecology of some Arctic foraminifera. Micropaleontology 61, 57-78.

Groot, D.E., Aagaard-Sørensen, S., Husum, K., 2014. Reconstruction of Atlantic water variability during the Holocene in the western Barents Sea. Climate of the Past 101, 51-62.

Hald, M., Korsun, S., 1997. Distribution of modern benthic foraminifera from fjords of Svalbard, European Arctic. Journal of Foraminiferal Research 272, 101-122.

Hald, M., Steinsund, P. I., 1996. Benthic foraminifera and carbonate dissolution in the surface sediments of the Barents and Kara Seas. Berichte zur Polarforschung, 212, 285-307.

Hammer, Ø., Harper, D.A.T., Ryan, P.D., 2001. PAST: Paleontological statistics software package for education and data analysis. Palaeontologia Electronica. 41, 9.

Harris, C. L., Plueddemann, A. J., Gawarkiewicz, G. G., 1998. Water mass distribution and polar front structure in the western Barents Sea. Journal of Geophysical Research: Oceans, 103(C2), 2905-2917.

Holbourn, A., Henderson, A.S., MacLeod, N., 2013. Atlas of benthic foraminifera. John Wiley & Sons. New York.

IPCC, 2019: Summary for Policymakers. In: IPCC Special Report on the Ocean and Cryosphere in a Changing Climate [H.-O. Pörtner, D.C. Roberts, V. Masson-Delmotte, P. Zhai, M. Tignor, E. Poloczanska, K. Mintenbeck, M. Nicolai, A. Okem, J. Petzold, B. Rama, N. Weyer (eds.)].

Jernas, P., Klitgaard-Kristensen, D., Husum, K., Koç, N., Tverberg, V., Loubere, P., Prins, M., Dijkstra, N., Gluchowska, M., 2018. Annual changes in Arctic fjord environment and modern benthic foraminiferal fauna: Evidence from Kongsfjorden, Svalbard. Global and Planetary Change 163, 119-140.

Jorissen, F.J., Wittling, I., 1999. Ecological evidence from live–dead comparisons of benthic foraminiferal faunas off Cape Blanc Northwest Africa. Palaeogeography Palaeoclimatology Palaeoecology 1491, 151-170.

Koenigk, T., Mikolajewicz, U., Jungclaus, J.H., Kroll, A., 2009. Sea ice in the Barents Sea: seasonal to interannual variability and climate feedbacks in a global coupled model. Climate dynamics 327-8, 1119-1138.

Koho, K.A., García, R.D., De Stigter, H.C., Epping, E., Koning, E., Kouwenhoven, T.J., Van der Zwaan, G.J., 2008. Sedimentary labile organic carbon and pore water redox control on species distribution of benthic foraminifera: A case study from Lisbon–Setúbal Canyon southern Portugal. Progress in Ocean. 791, 55-82.

Korsun, S., Hald, M., 1998. Modern benthic foraminifera off Novaya Zemlya tidewater glaciers, Russian Arctic. Arctic and Alpine Research, 30(1), 61-77.

Lantzsch, H., Hanebuth, T.J., Horry, J., Grave, M., Rebesco, M., Schwenk, T., 2017. Deglacial to Holocene history of ice-sheet retreat and bottom current strength on the western Barents Sea shelf. Quaternary Science Review. 173, 40-57.

Levin, L.A., 2005. Ecology of cold seep sediments: Interactions of fauna with flow, chemistry and microbes. Oceanography and Marine Biology 43, 1-46.

Licari, L.N., Schumacher, S., Wenzhofer, F., Zabel, M., Mackensen, A., 2003. Communities and microhabitats of living benthic foraminifera from the tropical east Atlantic: impact of different productivity regimes. Journal of Foraminiferal Research 331, 10-31.

Lind, S., Ingvaldsen, R.B., Furevik, T., 2018. Arctic warming hotspot in the northern Barents Sea linked to declining sea-ice import. Nature Climate Change 87, 634-639.

Loeblich, A.R., Tappan, H.N., 1953. Studies of Arctic foraminifera. Smithsonian Miscellaneous Collections, 121 (7), 1-150.

Loeblich, A.R., Tappan, H., 1988. Foraminiferal Genera and Their Classification. Van Nostrand Reinhold Co, New York, USA.

Loeng, H., 1991. Features of the physical oceanographic conditions of the Barents Sea. Polar Research. 101, 5-18.

Loeng, H., Ozhigin, V., Ådlandsvik, B., 1997. Water fluxes through the Barents Sea. ICES J. Marine Science. 543, 310-317.

Loubere, P., Jacobsen, B., Kristensen, D.K., Husum, K., Jernas, P., Richaud, M., 2011. The structure of benthic environments and the paleochemical record of foraminifera. Deep Sea Research. I 585, 535-545.

Lucchi, R.G., Bazzaro, M., Biebow, N., Carbonara, K., Caridi, F., De Vittor, C., Dominiczak, A., Gamboa Sojo, V.M., Graziani, S., Kovacevic, V., Krueger, M., Le Gall, C., Mazzini, A., Morigi, C., Musco, M.E., Povea, P., Relitti, F., Ruggiero, L., Rui, L., Sabbatini, A., Sánchez Guillamón, O., Tagliaferro, M., Topchiy, M., Wiberg, D., Zoch, D., with the collaboration of the scientific party of the Italian PNRA project DEFROST: Bensi, M.,

Deponte, D., Langone, L., Laterza, R., 2016. BURSTER - Bottom Currents in a Stagnant Environment, EUROFLEETS-2 Cruise Summary Report. 106. DOI: 10.13140/RG.2.2.24223.36004.

Maslowski, W., Marble, D., Walczowski, W., Schauer, U., Clement, J.L., Semtner, A.J., 2004. On climatological mass, heat, and SAL transports through the Barents Sea and Fram Strait from a pan-Arctic coupled ice-ocean model simulation, Journal of Geophysical Research, 109, C03032, doi:10.1029/2001JC001039.

Mau, S., Römer, M., Torres, M.E., Bussmann, I., Pape, T., Damm, E., Geprägs, P., Wintersteller, P., Hsu, C.W., Loher, M., Bohrmann, G., 2017. Widespread methane seepage along the continental margin off Svalbard-from Bjørnøya to Kongsfjorden. Scientific reports, 7(1), 1-13.

Murray, J.W., 2006. Ecology and applications of benthic foraminifera. Cambridge University Press, UK.

Murray, J. W., Alve, E., 1999. Natural dissolution of modern shallow water benthic foraminifera: taphonomic effects on the palaeoecological record. Palaeogeography, Palaeoclimatology, Palaeoecology, 146(1-4), 195-209.

Murray, J. W., Alve, E., 2016. Benthic foraminiferal biogeography in NW European fjords: A baseline for assessing future change. Estuarine, Coastal and Shelf Science, 181, 218-230.

Orvik, K.A., Niiler, P., 2002. Major pathways of Atlantic water in the northern North Atlantic and Nordic Seas toward Arctic. Geophysical Research Letters 2919, 2-1.

Peng, G., Steele, M., Bliss, A.C., Meier, W.N., Dickinson, S., 2018. Temporal Means and Variability of Arctic Sea Ice Melt and Freeze Season Climate Indicators Using a Satellite Climate Data Record, Remote Sensing. 2018, 10, 1328

Pittauerová, D., 2013. Gamma spectrometry for chronology of recent sediments. PhD thesis, Bremen University, 213.

Pucci, F., Geslin, E., Barras, C., Morigi, C., Sabbatini, A., Negri, A., Jorissen, F.J., 2009. Survival of benthic foraminifera under hypoxic conditions: Results of an experimental study using the CellTracker Green method. Marine Pollution Bulletin 598, 336-351.

Rathburn, A.E., Pérez, M.E., Martin, J.B., Day, S.A., Mahn, C., Gieskes, J., J., Ziebis, W., Williams, D., Bahls, A., 2003. Relationships between the distribution and stable isotopic composition of living benthic foraminifera and cold methane seep biogeochemistry in Monterey Bay, California. Geochemistry, Geophysics, Geosystems. 412.

Rebesco, M., Liu, Y., Camerlenghi, A., Winsborrow, M., Laberg, J.S., Caburlotto, A., Diviacco, P., Accettella, D., Sauli, C., Wardell, N., Tomini, I., 2011. Deglaciation of the western margin of the Barents Sea Ice Sheet—A swath bathymetric and sub-bottom seismic study from the Kveithola Trough. Marine Geology. 2791-4, 141-147.

Rebesco, M., Özmaral, A., Urgeles, R., Accettella, D., Lucchi, R.G., Rüther, D., Winsborrow, M., Llopart, J., Caburlotto, A., Lantzsch, H., Hanebuth, T.J., 2016. Evolution of a high-latitude sediment drift inside a glacially-carved trough based on high-resolution seismic stratigraphy Kveithola, NW Barents Sea. Quaternary Science Review. 147, 178-193.

Ritchie, J.C., McHenry, J.R., 1990. Application of radioactive fallout cesium-137 for measuring soil erosion and sediment accumulation rates and patterns: A review. Journal of Environmental Quality 192, 215-233.

Robbins, J.A., Edgington, D.N., 1975. Determination of recent sedimentation rates in Lake Michigan using Pb-210 and Cs-137. Geochimica et Cosmochimica Acta,393, 285-304.

Rüther, D.C., Bjarnadóttir, L.R., Junttila, J., Husum, K., Rasmussen, T.L., Lucchi, R.G., Andreassen, K., 2012. Pattern and timing of the northwestern Barents Sea Ice Sheet deglaciation and indications of episodic Holocene deposition. Boreas 413, 494-512.

Saher, M.H., Kristensen, D.K., Hald, M., Korsun, S., Jørgensen, L.L., 2009. Benthic foraminifera assemblages in the Central Barents Sea: an evaluation of combining live and total fauna studies in tracking environmental change. Norwegian Journal of Geology 89, 149-161

Saher, M., Kristensen, D.K., Hald, M., Pavlova, O., Jørgensen, L.L., 2012. Changes in distribution of calcareous benthic foraminifera in the central Barents Sea between the periods 1965–1992 and 2005–2006. Global and Planet. Change 98, 81-96.

Sakshaug, E., Slagstad, D., 1992 Sea ice and wind: Effects on primary productivity in the Barents Sea. Atmosphere-Ocean 30, 579-591.

Sarnthein, M., Van Kreveld, S., Erlenkeuser, H., Grootes, P.M., Kucera, M., Pflaumann, U., Schulz, M., 2003. Centennial-to-millennial-scale periodicities of Holocene climate and sediment injections off the western Barents shelf, 75° N. Boreas 323, 447-461.

Schlitzer, R., 2021. Ocean Data View, https://odv.awi.de.

Schröder, C.J., 1988. Subsurface preservation of agglutinated foraminifera in the northwest Atlantic Ocean. Abhandlungen der geologischen Bundesanstalt 41, 325-336.

Screen, J.A., Simmonds, I., 2010a. The central role of diminishing sea ice in recent Arctic temperature amplification. Nature 464 (7293), 1334-1337.

Screen, J.A., Simmonds, I., 2010b. Increasing fall-winter energy loss from the Arctic Ocean and its role in Arctic temperature amplification. Geophysical Research Letters 3716. L16707, doi:10.1029/2010GL044136.

Seidenkrantz, M. S., 1995. Cassidulina teretis Tappan and Cassidulina neoteretis new species (Foraminifera): stratigraphic markers for deep sea and outer shelf areas. Journal of Micropalaeontology, 14(2), 145-157.

Sejrup, H. P., Birks, H. J. B., Kristensen, D. K., Madsen, H., 2004. Benthonic foraminiferal distributions and quantitative transfer functions for the northwest European continental margin. Marine Micropaleontology, 53(1-2), 197-226.

Serreze, M.C., Holland, M.M., Stroeve, J., 2007. Perspectives on the Arctic's shrinking sea-ice cover. Science, 3155818, 1533-1536.

Ślubowska-Woldengen, M., Rasmussen, T.L., Koç, N., Klitgaard-Kristensen, D., Nilsen, F., Solheim, A., 2007. Advection of Atlantic Water to the western and northern Svalbard shelf since 17,500 cal yr BP. Quaternary Science Review 263-4, 463-478.

Smedsrud, L.H., Esau, I., Ingvaldsen, R.B., Eldevik, T., Haugan, P.M., Li, C., Lien, V.S., Olsen, A., Omar, A.M., Otterå, O.H., Risebrobakken, B., 2013. The role of the Barents Sea in the Arctic climate system. Review of Geophysics 513, 415-449.

Solomon, S., Manning, M., Marquis, M., Qin, D., 2007. Climate change 2007-the physical science basis: Working group I contribution to the fourth assessment report of the IPCC Vol. 4. Cambridge University Press, UK.

Steinsund, P. I., Polyak, L., Hald, M., Mikhailov, V., Korsun, S., 1994. Distribution of calcareous benthic foraminifera in recent sediments of the Barents and Kara Sea. Benthic Foraminifera in Surface Sediments of the Barents and Kara Seas: Modern and Late Quaternary Application. Ph. D. Thesis, Department of Geology, Institute of Biology and Geology, University of Tromsø, Norway.

Vinje, T., Kvambekk, Å.S., 1991. Barents Sea drift ice characteristics. Polar Research. 101, 59-68.

Wassmann, P., Martinez, R., Vernet, M., 1994. Respiration and biochemical composition of sedimenting organic matter during summer in the Barents Sea. Continental shelf research, 14(1), 79-90.

Wilson, L.J., Hald, M., Godtliebsen, F., 2011. Foraminiferal faunal evidence of twentieth-century Barents Sea warming. The Holocene 214, 527-537.

Wollenburg, J. E., Mackensen, A., 1998. Living benthic foraminifers from the central Arctic Ocean: faunal composition, standing stock and diversity. Marine Micropaleontology. 343-4, 153-185.

Yang, X. Y., Wang, G., Keenlyside, N., 2020. The Arctic sea ice extent change connected to Pacific decadal variability. Cryosphere 14, 693–708.

Zaborska, A., Carroll, J., Papucci, C., Torricelli, L., Carroll, M. L., Walkusz-Miotk, J., Pempkowiak, J., 2008. Recent sediment accumulation rates for the Western margin of the Barents Sea. Deep Sea Research. II 5520-21, 2352-2360.

Do not remove this file (contains research data)

Click here to access/download
RDM Data Profile XML
DataProfile_5639152.xml

Author contributions

R.G.L. and **C.M.** conceived and designed the research. **R.G.L.** PI of BURSTER project. **C.M.** PI of AXED project and conceptualization. **V.M.G.S., F.C., A.S., R.G.L., M.B., V.K., A.T.D., P.P., C.M.** acquired data at sea during the BURSTER cruise. **V.M.G.S.** processed and analysed the dead foraminiferal assemblages and living data ≥150 µm. **V.M.**, **C.M.** and **K.H.** analysed the dead foraminiferal assemblages data. **F.C.** and **A.S.** processed and analysed the living foraminiferal assemblages. **R.G.L.** processed sedimentological data. **M.B., V.K.** processed and analysed oceanographic data. **A.T.D.** processed ^{210}Pb and ^{137}Cs radionuclide measurements. **L.L.** and **A.T.D.** calculated ^{210}Pb-based sedimentation rates**. P.P.** carried out grain size analysis. **V.M.G.S**. wrote the most of the manuscript with contributions from: **C.M.** and **K.H.** dead foraminiferal assemblages, preservation and taphonomic processes; **F.C.** and **A. S.** Living foraminiferal assemblages and modern situation; **R.G.L.** grain size and sedimentological analyses; **M.B.** and **V.K.** oceanographic data and water masses properties; **L.L.** and **A.T.D.** age model and sedimentation rate. All authors discussed the results, the conclusions and reviewed the manuscript.

Click here to access/download
Supplementary Material
Splementary material.docx